Activation of Slo2.1 channels by niflumic acid

Li Dai, Vivek Garg, and Michael C. Sanguinetti

Department of Physiology, Nora Eccles Harrison Cardiovascular Research and Training Institute, University of Utah, Salt Lake City, UT 84112

Slo2.1 channels conduct an outwardly rectifying K^+ current when activated by high $[Na^+]_i$. Here, we show that gating of these channels can also be activated by fenamates such as niflumic acid (NFA), even in the absence of intracellular Na^+. In *Xenopus* oocytes injected with <10 ng cRNA, heterologously expressed human Slo2.1 current was negligible, but rapidly activated by extracellular application of NFA (EC_{50} = 2.1 mM) or flufenamic acid (EC_{50} = 1.4 mM). Slo2.1 channels activated by 1 mM NFA exhibited weak voltage dependence. In high $[K^+]_e$, the conductance–voltage (G-V) relationship had a $V_{1/2}$ of +95 mV and an effective valence, *z*, of 0.48 *e*. Higher concentrations of NFA shifted $V_{1/2}$ to more negative potentials (EC_{50} = 2.1 mM) and increased the minimum value of G/G_{max} (EC_{50} = 2.4 mM); at 6 mM NFA, Slo2.1 channel activation was voltage independent. In contrast, $V_{1/2}$ of the G-V relationship was shifted to more positive potentials when $[K^+]_e$ was elevated from 1 to 300 mM (EC_{50} = 21.2 mM). The slope conductance measured at the reversal potential exhibited the same $[K^+]_e$ dependency (EC_{50} = 23.5 mM). Conductance was also $[Na^+]_e$ dependent. Outward currents were reduced when Na^+ was replaced with choline or mannitol, but unaffected by substitution with Rb^+ or Li^+. Neutralization of charged residues in the S1–S4 domains did not appreciably alter the voltage dependence of Slo2.1 activation. Thus, the weak voltage dependence of Slo2.1 channel activation is independent of charged residues in the S1–S4 segments. In contrast, mutation of R190 located in the adjacent S4–S5 linker to a neutral (Ala or Gln) or acidic (Glu) residue induced constitutive channel activity that was reduced by high $[K^+]_e$. Collectively, these findings indicate that Slo2.1 channel gating is modulated by $[K^+]_e$ and $[Na^+]_e$, and that NFA uncouples channel activation from its modulation by transmembrane voltage and intracellular Na^+.

INTRODUCTION

Intracellular Na^+-activated K^+ (K_{Na}) channels have a large conductance (150–180 pS with $[K^+]_e$ of 140 mM) and a very low open probability (P_o) under normal physiological and ionic conditions, but they are rapidly activated upon elevation of $[Na^+]_i$, with an EC_{50} of ~30 mM (Kameyama et al., 1984). Weakly voltage-dependent K_{Na} channel currents have been recorded from neurons (Bader et al., 1985; Haimann and Bader, 1989; Haimann et al., 1990, 1992; Egan et al., 1992b; Dryer, 1994; Zhainazarov and Ache, 1997) and cardiac myocytes (Kameyama et al., 1984; Luk and Carmeliet, 1990; Rodrigo and Chapman, 1990; Sanguinetti, 1990). It has been proposed that activation of cardiac K_{Na} channels during ischemia has a protective role by shortening action potential duration and preventing Ca^{2+} overload (Kameyama et al., 1984; Sanguinetti, 1990; Wang et al., 1991).

The molecular cloning in 2003 of two genes named Slo2.1 ("Slick") (Bhattacharjee et al., 2003) and Slo2.2 ("Slack") (Bhattacharjee et al., 2003; Yuan et al., 2003) based on their homology to Slo1 (BK or $K_{Ca1.1}$), has enabled molecular studies of K_{Na} channels not previously possible. The various Slo K^+ channels are regulated by binding of distinct intracellular ions to a cytosolic C-terminal domain: Ca^{2+} for Slo1 (Adelman et al., 1992), Na^+ for Slo2, and H^+ for Slo3 (Schreiber et al., 1998). The study of heterologously expressed Slo2.1 channels revealed that in addition to the anticipated role of $[Na^+]_i$, these channels are also activated by intracellular Cl^- and inhibited by 5 mM of intracellular ATP (Bhattacharjee et al., 2003). ATP-sensitive K^+ channels are inhibited by lower $[ATP]_i$ (Noma, 1983); however, it is unclear whether the decreased $[ATP]_i$ or elevated $[Na^+]_i$ associated with ischemic conditions leads to a preferential early activation of either K_{Na} or ATP-sensitive K^+ channels. The conductance and gating properties of K^+-selective channels can also be modified by the concentrations of $[Na^+]_e$ and $]K^+]_e$. Extracellular Na^+ enhances the conductance of inward rectifier K^+ channels (Ohmori, 1978), and the conductance and gating of Kv channels is $[K^+]_e$ dependent. Multi-ion barrier models (Hille and Schwarz, 1978) predict that single-channel conductance saturates at high levels of $[K^+]_e$, and C-type inactivation of voltage-gated K^+ (Kv) channels is reduced

Correspondence to Michael C. Sanguinetti: sanguinetti@cvrti.utah.edu

Abbreviations used in this paper: FFA, flufenamic acid; GHK, Goldman-Hodgkin-Katz; K_{Na}, intracellular Na^+-activated K^+; NFA, niflumic acid; PH, pore helix; P_o, open probability; SF, selectivity filter; VSD, voltage sensor domain; WT, wild-type.

The Rockefeller University Press $30.00
J. Gen. Physiol. Vol. 135 No. 3 275–295
www.jgp.org/cgi/doi/10.1085/jgp.200910316

at elevated $[K^+]_e$ (Baukrowitz and Yellen, 1995). The effects of $[Na^+]_e$ and $[K^+]_e$ on Slo2.1 channel currents have not been previously investigated.

Fenamates such as niflumic acid (NFA) were developed for use as nonsteroidal antiinflammatory agents. In addition to their antiinflammatory activity, these compounds also affect ion channels at high (mM) concentrations. The fenamates were first shown to block Cl^- channels (White and Aylwin, 1990) and were later reported to alter the gating of a wide spectrum of ion channel types (Busch et al., 1994; H.S. Wang et al., 1997; Malykhina et al., 2002; Peretz et al., 2005; Fernandez et al., 2008). The most dramatic effect of fenamates on ion channels is their activation of Slo1. When applied to the extracellular chamber, 1 mM NFA caused an approximately fivefold increase in P_o of coronary smooth muscle BK channels reconstituted in bilayers (Ottolia and Toro, 1994), and 0.5 mM NFA induced a threefold increase in currents conducted by heterologously expressed human Slo1 channels (Gribkoff et al., 1996). The effects of fenamates on other members of the Slo channel family have not been reported.

The S1–S4 α-helical transmembrane segments comprise the voltage sensor domain (VSD) in voltage-gated K^+, Na^+, and Ca^{2+} channels. The S4 segment is the primary voltage sensor, but acidic residues in the S2 and S3 segments can also form charge pair interactions with basic residues in S4, and these interactions are important for subunit folding or voltage sensor function (Seoh et al., 1996; Tiwari-Woodruff et al., 1997, 2000). The net charge of the S4 segment in Shaker, the prototypical Kv channel is +7. Slo1 has only three basic residues in the S4, and the functional voltage sensor of Slo1 channels is proposed to be composed of four charged residues: one in S4 (R213), two in S2 (D153, R167), and one in S3 (D186), based on the ability of charge-altering mutations to reduce the voltage dependence of P_o (Ma et al., 2006). The charge displacement associated with full activation of a Slo1 channel is estimated to be only 2.6 *e* (Horrigan et al., 1999), several times smaller than the 13 *e* estimated for Shaker (Aggarwal and MacKinnon, 1996). In contrast to Slo1 and typical Kv channels, the S4 of Slo2.1 has only two basic charges, and these are offset by two acidic residues to give a net charge of 0. Based on the paucity of positive charge and the neutral net charge, it seems unlikely that the S4 of Slo2.1 could effectively sense transmembrane voltage or play an important role in coupling cell depolarization to channel activation. However, Slo2.1 also has several other basic and acidic residues in S1–S3, and some of these alone, or in concert with one or more of the charged residues in S4, could comprise a voltage-sensing module.

Here, we show that dormant Slo2.1 channels can be markedly activated by extracellular applied NFA, rivaling and superseding the effect of elevated $[Na^+]_i$. Slo2.1 channels were heterologously expressed in *Xenopus* oocytes, and currents activated by NFA were characterized using two-microelectrode voltage clamp and patch clamp techniques. We also characterize the weak voltage dependence of Slo2.1 channel gating as a function of [NFA] and $[K^+]_e$, and determine the effect of substitution of extracellular Na^+ with other monovalent cations. Finally, the structural basis of voltage-dependent gating was explored by mutating the charged residues in segments S1–S4, the consensus voltage-sensing domain of Kv channels.

MATERIALS AND METHODS

Molecular biology

The human *Slo2.1* full-length cDNA (GenBank accession no. NM_198503) fragment was isolated by EcoRV and SpeI digestion from hSlick/pTRACER plasmid (provided by L. Kaczmarek, Yale University, New Haven, CT) and subcloned into the psGEM oocyte expression vector. Mutations of wild-type (WT) *hSlo2.1* cDNA were performed using the Quickchange site-directed mutagenesis kit (Agilent Technologies). Mutation constructs were confirmed by restriction enzyme and DNA sequence analyses. Complementary RNAs (cRNA) was prepared with mMessage mMachine T7 (Applied Biosystems) after linearization of the expression construct with SfiI. The concentration of cRNA was quantified by spectroscopy or with the RiboGreen assay (Invitrogen).

Oocyte isolation and cRNA injection

The procedures used to harvest oocytes from *Xenopus laevis* were approved by the University of Utah Institutional Animal Care and Use Committee. Frogs were anesthetized with 0.2% tricaine methane sulfonate in deionized water before a small abdominal incision was made to remove ovarian lobes. The incision was sutured closed, and the frog was returned to its aquarium for a recovery period of at least 1 mo before the procedure was repeated. After a maximum of three surgical procedures, tricaine-anaesthetized frogs were killed by pithing. Oocytes were manually dispersed from the lobes, and the follicle cell layer was removed by treatment for 90–150 min with 1 mg/ml of type II collagenase (Worthington) in ND96-Ca^{2+}–free solution that contained (in mM): 96 NaCl, 2 KCl, 1 $MgCl_2$, and 5 HEPES; pH was adjusted to 7.6 with NaOH.

To characterize Slo2.1 channel current ($I_{Slo2.1}$), stage IV and V oocytes were injected with 0.2–6 ng of WT or mutant human *Slo2.1* cRNA. Oocytes were subsequently stored for 1–3 d at 18°C in Barth's saline solution that contained (in mM): 88 NaCl, 1 KCl, 0.41 $CaCl_2$, 0.33 $Ca(NO_3)_2$, 1 $MgSO_4$, 2.4 $NaHCO_3$, 10 HEPES, and 1 pyruvate plus 50 mg/L gentamycin; pH was adjusted to 7.4 with NaOH.

Two-electrode voltage clamp

1–3 d after injection with cRNA, oocytes were placed in a 0.2-ml recording chamber and perfused at 2 ml min^{-1} with KCM211 solu tion at room temperature (22–24°C). Standard two-microelectrode voltage clamp techniques were used to record ionic currents from single oocytes (Goldin, 1991; Stühmer, 1992). A GeneClamp 500 amplifier, Digidata 1322A data acquisition system, and Clampex 8.2 or 9.0 software (MDS Analytical Technologies) were used to produce command voltages and to record current and voltage signals. I-V relationships for WT and mutant channels were determined by measuring currents at the end of test pulses applied in 20-mV increments to potentials that usually ranged from −160

to +80 (or +120) mV. Unless otherwise specified, the holding potential (V_h) or prepulse was −80 mV and the interpulse interval was 10 s. Other voltage pulse protocols are described in Results and the figure legends.

Single-channel recording

The activity of multiple Slo2.1 channels was measured in cell-attached and inside-out patches of oocyte membrane using the patch clamp technique (Hamill et al., 1981). Manual removal of the vitelline membrane from single oocytes was facilitated by treatment for 2–5 min with a hypertonic solution that contained (in mM): 200 K aspartate, 20 KCl, 1 $MgCl_2$, 1 EGTA, and 10 HEPES, pH 7.4. Patch pipettes were fabricated from borosilicate glass (Sutter Instrument Co.) and had a resistance of 8–13 MΩ when filled with the pipette solution. Currents were recorded using an Axopatch 200B amplifier, on-line filtered at 1 kHz using an eight-pole Bessel filter, and digitized at 5 kHz. Currents were elicited using voltage ramps or were recorded continuously (gap-free) for several minutes at a variable test potential (V_t) to determine i-V relationships.

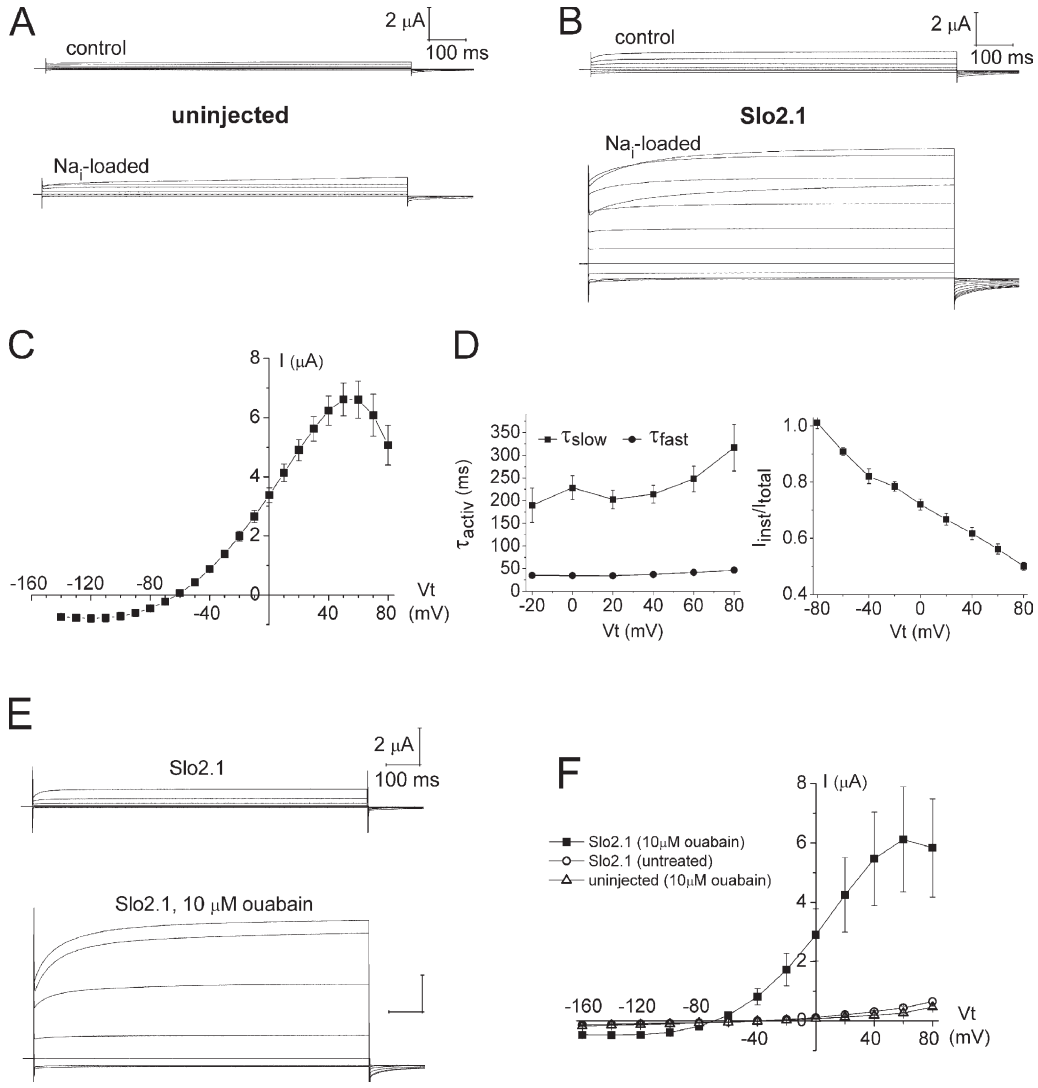

Figure 1. Incubation of oocytes with Na_i-loading solution activates $I_{Slo2.1}$. (A) Currents recorded from an uninjected oocyte before (control) and after 10-min incubation in Na_i-loading solution. V_t was varied from −140 to +80 mV and applied in 20-mV increments from a holding potential of −80 mV. (B) Currents recorded from an oocyte injected with 3.2 ng *Slo2.1* cRNA before (control) and after incubation in Na_i-loading solution for 10 min. V_t was varied from −140 to +80 mV and applied in 20-mV increments from a holding potential of −80 mV. (C) Average $I_{Slo2.1}$–V relationship determined after incubation of oocytes in Na_i-loading solution for 10–15 min ($n = 8$). (D) Kinetics of $I_{Slo2.1}$ activated by incubation of oocytes with Na_i-loading solution for 15 min. Left plot summarizes the fast and slow time constants for activation (τfast and τslow) of the time-dependent component of current ($n = 15$). On the right is a plot of the amplitude of the instantaneous current (I_{inst}) divided by the total outward current (I_{total}) ($n = 15$). (E) Currents recorded from oocytes injected with 3.2 ng *Slo2.1* cRNA and incubated in Barth's solution (top) or Barth's solution plus 10 μM ouabain for 2 d (bottom). V_t was varied from −160 to +80 mV, applied in 40-mV increments. (F) I-V relationships for uninjected oocytes incubated in Barth's solution plus 10 μM ouabain for 2 d (open triangle; $n = 9$) and in oocytes injected with 3.2 ng Slo2.1 cRNA and incubated in Barth's solution alone (open circle; $n = 7$) or in Barth's solution plus 10 μM ouabain for 2 d (filled square; $n = 13$).

Solutions and drugs

For two-microelectrode voltage clamp recording, all extracellular solutions contained 1 $CaCl_2$, 1 $MgCl_2$, and 5 mM HEPES, along with a variable concentration of KCl and NaCl. KCM211 external solution contained (in mM): 98 NaCl, 2 KCl, 1 $CaCl_2$, 1 $MgCl_2$, and 5 mM HEPES; pH was adjusted to 7.6 with NaOH. KCM411 was the same, except for KCl (4 mM) and NaCl (96 mM). K104 solution contained 104 mM KCl, 0 NaCl, 1 $CaCl_2$, 1 $MgCl_2$, and 1 mM HEPES. To increase $[Na^+]_i$ and activate Slo2.1 channels, the Na^+ pump was inhibited by incubating oocytes for 5–20 min in a Na_i-loading extracellular solution that contained (in mM): 110 NaCl, 2.5 Na citrate, and 5 MOPS, pH 7.6. Using this solution, the $[Na^+]_i$ in oocytes can reach a level of 80 mM after 2 h of incubation (Vasilets et al., 1991). The Na_i-loading solution was washed out and replaced with KCM211 external solution plus 10 µM ouabain immediately before recording currents.

For cell-attached and inside-out patch recording of single-channel activity, the pipette (extracellular) solution contained (in mM): K gluconate and Na gluconate (as indicated for specific experiments), 2 $MgCl_2$, 0.1 $CaCl_2$, and 10 HEPES, pH 7.2. To activate Slo2.1 channels, NFA (1–6 mM) was also added to the pipette solution. For inside-out patch recordings, oocytes were bathed in an "intracellular" solution that contained (in mM): variable KCl and NaCl as indicated, 2 $MgCl_2$, 10 HEPES, and 2 EGTA, pH 7.2.

NFA and flufenamic acid (FFA) were purchased from Sigma-Aldrich and dissolved in dimethyl sulfoxide as a 1-M stock solution. For some experiments, the Na^+ pump was inhibited by incubation of oocytes with ouabain (Sigma-Aldrich) at a concentration of 10 µM. All solutions containing NFA were corrected to pH 7.6 with NaOH or KOH.

Data analysis

Off-line data analysis was performed with Clampfit 8.2 or 9.0 (MDS Analytical Technologies), Origin 7.5 (OriginLab), and Excel (Microsoft) software. All data are expressed as mean ± SEM (n = number of oocytes). $I_{Slo2.1}$ was plotted as a function of V_t to obtain an I-V relationship. Relative conductance (G/G_{max}) was calculated as $I_{Slo2.1}/(V_t - E_{rev})$, where E_{rev} is the reversal potential of whole cell current, and plotted as a function of V_t for each oocyte. The relationship was fitted to a Boltzmann function, and G_{max} was estimated by extrapolation of the curve to more positive potentials. The resulting normalized G-V relationships were again fitted with a Boltzmann function (Eq. 1), where z is the effective valence, F is Faraday's constant, R is the gas constant, T is room temperature in °K, and $V_{1/2}$ is the potential at which the current is half-activated.

$$G / G_{max} = 1 / \{1 + \exp[2zF / RT(V_t 2V_{1/2})]\} \quad (1)$$

The amplitude of single-channel currents was determined from all-points histograms of channel activity when the potential was held at a constant level for 1–2 min.

The concentration–effect relationship for NFA activation of $I_{Slo2.1}$ measured at a single V_t was fitted with a Hill equation (Eq. 2). EC_{50} is the [NFA] that produced a half-maximal response, and n_H is the Hill coefficient.

$$I_{Slo2.1} / I_{Slo2.1max} = [NFA]^{nH} / \left([NFA]^{nH} + EC_{50}{}^{nH}\right) \quad (2)$$

A modified Hill equation (Eq. 3) was used to estimate EC_{50} and n_H for NFA-mediated effects on $V_{1/2}$ of activation or slope conductance, where A_1 and A_2 are the minimum and maximum values of the parameter measured. The coefficient of determination (R^2) for goodness of fit is also provided.

$$y = A_1 + (A_2 - A_1) \bullet [NFA]^{nH} / \left(EC_{50}{}^{nH} + [NFA]^{nH}\right) \quad (3)$$

RESULTS

Activation of Slo2.1 channels by intracellular Na^+ loading

Under normal physiological conditions, Slo2.1 channel currents were very small or undetectable in oocytes studied 3 d after injection with <10 ng of human *Slo2.1*

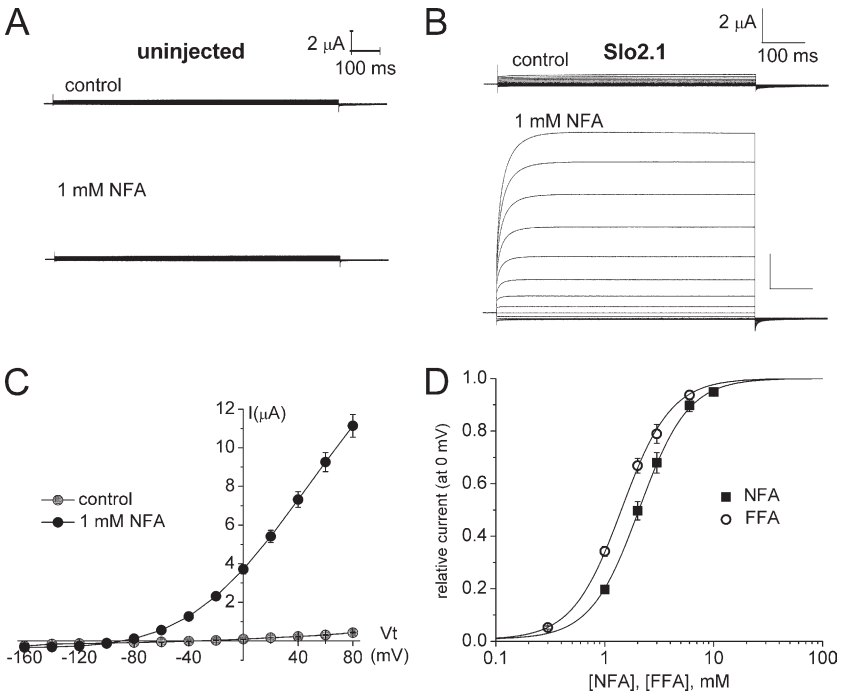

Figure 2. NFA activates Slo2.1 channels heterologously expressed in oocytes. (A) Currents recorded from an uninjected oocyte before and after treatment with 1 mM NFA. (B) Currents recorded from an oocyte expressing Slo2.1 before (control) and after treatment with 1 mM NFA for 8 min. Oocytes were injected 2 d earlier with 0.32 ng Slo2.1 cRNA. In A and B, V_t was varied from −160 to +80 mV, applied in 20-mV increments. (C) Average I-V relationships for currents recorded before (control) and after treatment with 1 mM NFA (n = 35). (D) [NFA]– and [FFA]–response relationships for increase of $I_{Slo2.1}$ in response to continuous pulsing to 0 mV. Data were fitted with a Hill equation (smooth curves) to determine EC_{50} (2.08 ± 0.04 mM) and Hill coefficient, n_H (1.94 ± 0.05), for NFA (n = 12). For FFA, the EC_{50} was 1.4 ± 0.02 mM and n_H was 1.92 ± 0.03 (n = 5).

cRNA. As reported previously (Santi et al., 2006), functional Slo2.1 channel expression in oocytes was achieved after injection of large amounts (75 ng/oocyte) of cRNA. The lack of functional Slo2.1 channel expression in oocytes injected with low amounts of cRNA is likely due to the low probability of channel opening when $[Na^+]_i$ is within its normal physiological range of 4–10 mM (Weber, 1999). $[Na^+]_i$ in *Xenopus* oocytes can be elevated by bathing the cells in a Na_i-loading solution that inhibits the Na^+ pump and gradually leads to an accumulation of intracellular Na^+ ions (Vasilets et al., 1991). In uninjected oocytes, Na_i loading for 10–15 min enhanced outward currents about twofold (Fig. 1 A), consistent with an activation of endogenous K_{Na} channels (Egan et al., 1992a). In contrast, in oocytes injected with 3.2 ng/oocyte of *Slo2.1* cRNA, current magnitude was enhanced ~10-fold after Na_i loading (Fig. 1 B). The I-V relationship for $I_{Slo2.1}$ exhibited the typical pattern of outward rectification expected for K_{Na} channels (Fig. 1 C). In addition, the slope conductance was negative for V_t > +50 mV. The negative slope conductance at positive potentials is likely caused by block of outward currents by the elevated $[Na^+]_i$, as reported previously for single K_{Na} channels in guinea pig myocytes (Wang et al., 1991).

The activation of Slo2.1 current exhibited two components. At the more negative potentials, the onset of outward current was instantaneous or at least reached a steady-state level within the time course of the capacitance transient (τ ~1 ms). At a V_t positive to −60 mV, an additional time-dependent component of activation was observed. The onset of this later component was best described by a bi-exponential function with time constants of ~35 and ~200 ms (Fig. 1 D, left). The fraction of instantaneous to total current varied from 1.0 at −80 mV to 0.5 at +80 mV (Fig. 1 D, right). As reported previously for native K_{Na} channels in guinea pig myocytes (Luk and Carmeliet, 1990), $I_{Slo2.1}$ could also be activated by incubation of oocytes with ouabain (Fig. 1, E and F). Thus, $I_{Slo2.1}$ is readily activated by increasing $[Na^+]_i$ secondary to an inhibition of the Na^+ pump.

Activation of Slo2.1 by fenamates

Fenamates such as NFA were originally reported to block Cl^- channels (White and Aylwin, 1990), but have since been reported to also alter the gating of a wide spectrum of ion channel types (Busch et al., 1994; H.S. Wang et al., 1997; Malykhina et al., 2002; Peretz et al., 2005; Fernandez et al., 2008). At 1 mM, extracellularly applied NFA caused an approximate fivefold increase in P_o of coronary smooth muscle BK channels reconstituted in bilayers (Ottolia and Toro, 1994), and 0.5 mM induced a threefold increase in currents conducted by heterologously expressed human Slo1 channels (Gribkoff et al., 1996). We found that NFA also activates Slo2.1 channels (Fig. 2). NFA at 1 mM caused only a slight change in the magnitude of endogenous currents (Fig. 2 A). However, in oocytes expressing Slo2.1, the drug induced a very large increase in current magnitude (Fig. 2 B). The onset of current increase was very rapid, commencing immediately after switching the perfusate from the control solution to one containing 1 mM NFA. In oocytes injected with 0.84 ng cRNA, 1 mM NFA induced an 80-fold increase in the magnitude of outward current measured at 0 mV (n = 11). Unlike Slo2.1 channels activated by treatment with the Na_i-loading solution, the I-V relationship for NFA-activated channels (Fig. 2 C) did not exhibit a reduced slope conductance at potentials >+40 mV, presumably because $[Na^+]_i$ was not altered by NFA.

When quantified by repetitive pulsing to 0 mV, the effects of NFA were concentration dependent over the range of 1 to 10 mM, with an EC_{50} of 2.08 ± 0.04 mM (Fig. 2 D; n = 12). A related fenamate, FFA, was also an effective activator of Slo2.1 channels, with an EC_{50} of 1.43 ± 0.02 mM (Fig. 2 D; n = 5). The Hill coefficient (n_H) for both fenamates was 1.9, indicating a positively cooperative binding reaction.

The activation of Slo2.1 by Na_i loading or NFA was compared in a single oocyte (Fig. 3). Currents were recorded at potentials ranging from −160 to +100 mV under control conditions (KCM211 external solution) and after treatment with 1 mM NFA (Fig. 3 A, *a* and *b*). The I-V

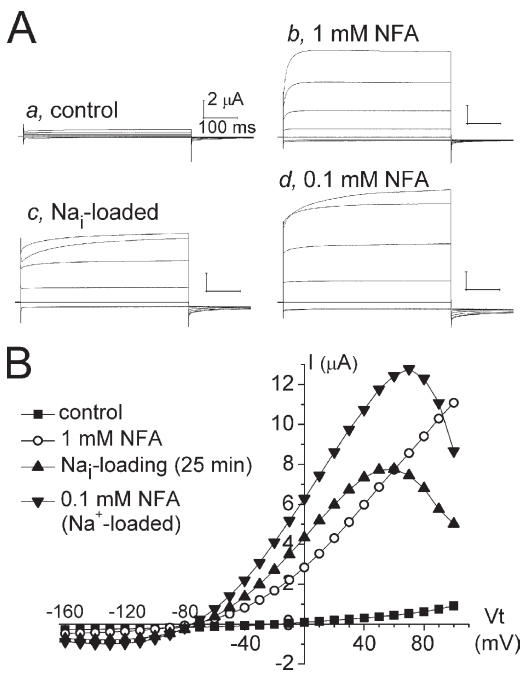

Figure 3. Increased $[Na^+]_i$ blocks outward $I_{Slo2.1}$ at positive potentials. (A) Currents recorded from an oocyte expressing Slo2.1 under control conditions (*a*) after 8-min treatment with 1 mM NFA (*b*), after 25-min incubation in Na_i-loading solution (*c*), and then after 8-min treatment with 0.1 mM NFA (*d*). V_t was varied from −160 to +80 mV and applied in 40-mV increments. (B) I-V relationships for the oocyte under the indicated conditions.

relationship was linear at positive potentials in the presence of NFA (Fig. 3 B). The same cell was then incubated in the Na_i-loading solution without NFA for 25 min. The currents recorded after Na_i loading activated more slowly at positive potentials (Fig. 3 A, *c*), and the I-V relationship exhibited a region of negative slope conductance at potentials positive to +50 mV (Fig. 3 B). Although subsequent addition of 0.1 mM NFA further increased current magnitude (Fig. 3 A, *d*), the nonlinearity of the I-V relationship persisted (Fig. 3 B). Collectively, these findings suggest that although an increase in $[Na^+]_i$ activates Slo2.1 channels, it also causes a voltage-dependent pore block at potentials positive to +40 mV, the approximate reversal potential for Na^+. The uncertainty regarding the absolute change in $[Na^+]_i$ induced by treatment of oocytes with the Na_i-loading solution limits the utility of this approach to study Slo2.1. In contrast, treatment of oocytes expressing Slo2.1 channels with NFA is a rapid and reproducible method to activate whole cell channel current, and this method was used for the remaining studies.

Single Slo2.1 channel activity was readily recorded in cell-attached patches if the pipette solution contained a high $[K^+]$ and NFA. Without NFA in the pipette, single-channel activity was not observed. In the example shown in Fig. 4 A, the pipette solution contained 2 mM NFA, and only one channel was evident in the cell-attached patch when the voltage was ramped from +60 to −120 mV (Fig. 4 A, *i*). Note that the P_o was much higher at positive potentials compared with negative potentials. Excision of the patch to form an inside-out configuration into a bathing ("cytosolic") solution that contained 140 KCl increased channel activity and revealed the presence of two channels in the patch (Fig. 4 A, *ii*). This increase in channel activity upon patch excision was observed in seven additional patches and may be caused by the absence of ATP and/or the higher concentration of Cl^- in the bathing solution compared with the cytosol. Intracellular ATP blocks, whereas Cl^- activates, Slo2.1 channels (Bhattacharjee et al., 2003). Switching the bathing solution to one containing 80 mM NaCl and 60 mM KCl increased

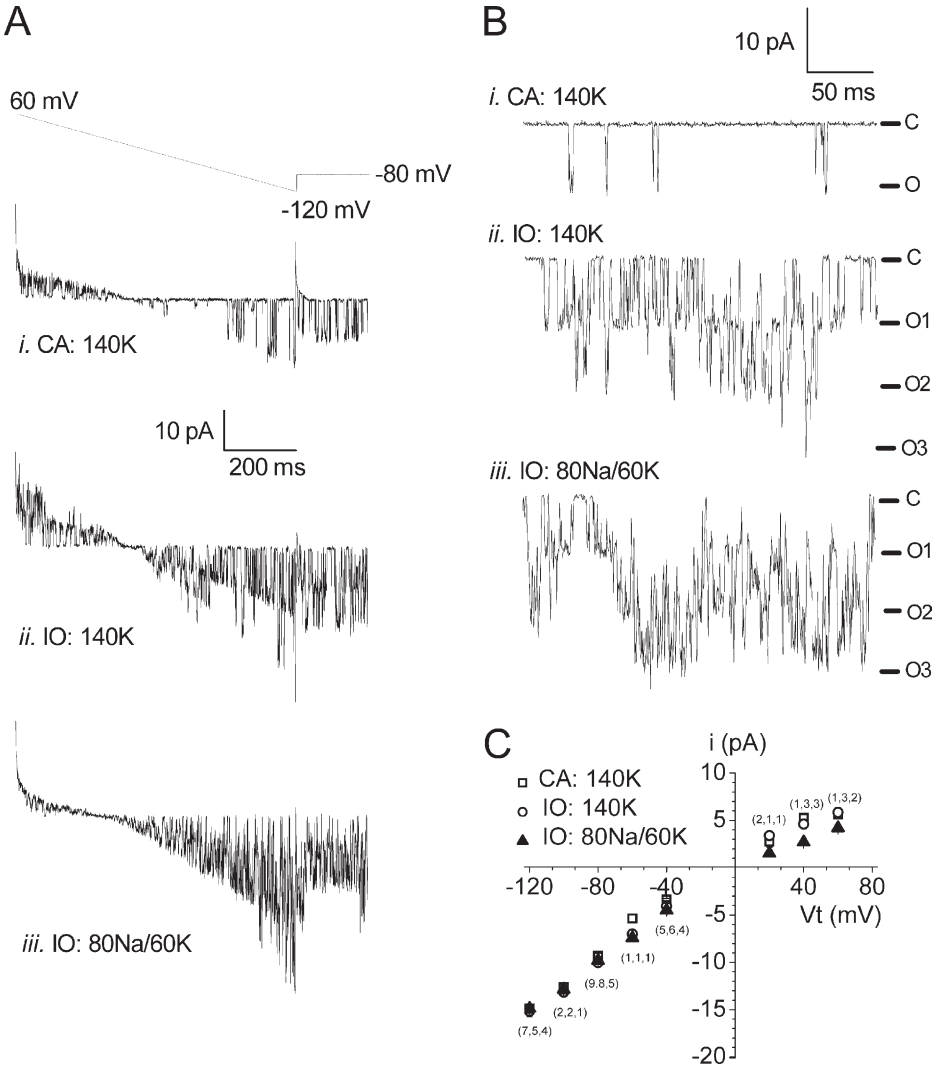

Figure 4. Activation of single Slo2.1 channels by extracellular NFA and intracellular Na^+. (A) Slo2.1 channels recorded during voltage ramp from +60 to −120 mV. The top panel illustrates voltage clamp protocol. Currents were recorded from a single patch under three recording conditions: cell-attached (CA) patch mode (*i*) or inside-out (IO) mode (*ii*) with a bath solution that contained 140 mM KCl, and inside-out mode (*iii*) with a bath solution that contained 80 mM NaCl and 60 mM KCl. (B) Slo2.1 channel activity measured during gap-free recordings at –80 mV from the same patch as in A. The closed (C) and open (O1, O2, and O3) state levels are indicated to the right of the current traces. (C) Single-channel i-V relationships for the three recording conditions as indicated. Numbers in parenthesis indicate the number of patches summarized for each data point in the order indicated by the inset legend. The slope conductance for single channels (γ) determined for −40 to −120 mV was 144 ± 8 pS for CA patches, 144 ± 6 pS for IO patches and 140 KCl bath solution, and 130 ± 7 pS for IO patches and 80 NaCl/60 KCl bath solution.

channel activity and revealed that the patch contained at least three channels, two of which were apparently silent when currents were measured in the cell-attached patch mode (Fig. 4 A, *iii*). As expected, the outward currents were reduced when the bath solution was switched from 140 mM KCl to 60 mM KCl/80 mM NaCl because of the change in E_{rev} and the accompanying reduction in driving force for K^+. As reported previously for inside-out patch recordings of heterologously expressed Slo2.1 channels (Yuan et al., 2003) or native K_{Na} channels (Kameyama et al., 1984; Niu and Meech, 2000), Slo2.1 exhibited reduced voltage dependence when recorded using high $[K^+]_e$ and high $[Na^+]_i$. Channel activity was also measured using gap-free recording in this patch under the three recording conditions (Fig. 4 B); here, the difference in the number of active channels in the patch and P_o is even more evident. The amplitude of single-channel currents (Fig. 4 B, *i*) was determined from analysis of all-points amplitude histograms at each potential to construct the i-V relationships shown in Fig. 4 C. Thus, Slo2.1 channels are activated independently by extracellular NFA and intracellular Na^+.

To determine the concentration-dependent agonist activity of NFA over a wide range of test potentials, oocytes were injected with a small amount of cRNA (0.2 ng/oocyte) to limit the size of currents evoked with higher drug concentrations. The increase in the magnitude of $I_{Slo2.1}$ by 1, 3, and 6 mM NFA was both concentration and voltage dependent (Fig. 5 A). The maximum slope conductance, g_{max} $[(dI_{Slo2.1}/dV_t)_{max}]$, was 51 μS at 1 mM, 103 μS at 3 mM, and 142 μS at 6 mM NFA. The G-V relationships (Fig. 5 B) were determined for each concentration of NFA by dividing peak $I_{Slo2.1}$ values from the I-V relationship by the electrical driving force $(V_t - E_{rev})$. At 1 mM NFA, the average $V_{1/2}$ value of the G-V relationship for this group of oocytes was -1.5 ± 0.7 mV, and the slope factor was 36 mV, equivalent to a z value of 0.71 ± 0.01 e ($n = 8$). The $V_{1/2}$ for activation was shifted by -42 mV when [NFA] was increased from 1 to 3 mM NFA and by -83 mV with 6 mM NFA (Fig. 5 B; $n = 5$–7). The equivalent valence, z, decreased from an average of 0.71 at 1 mM to 0.57 at 3 mM and 0.46 at 6 mM NFA. Thus, NFA stabilized the open state of Slo2.1 channels in a concentration-dependent manner.

Similar to current activated by the Na_i-loading solution, $I_{Slo2.1}$ activated by NFA exhibited an instantaneous and a time-dependent component. The time-dependent component became apparent at a $V_t > -60$ mV, and its bi-exponential onset was [NFA] dependent (Fig. 5 C). The time-dependent component of current induced by NFA was faster in onset when compared with current activated by elevated $[Na^+]_i$. For example, at +80 mV, the fast and slow time constants for the onset of time-dependent current were ~5 and 17 ms with 1 mM NFA, compared with 50 and 325 ms for current activated by elevated $[Na^+]_i$. Similar to $I_{Slo2.1}$ induced by Na_i loading, the ratio of instantaneous to total $I_{Slo2.1}$ (I_{inst}/I_{total}) activated by NFA was 1.0 at -80 mV and was decreased as V_t was made

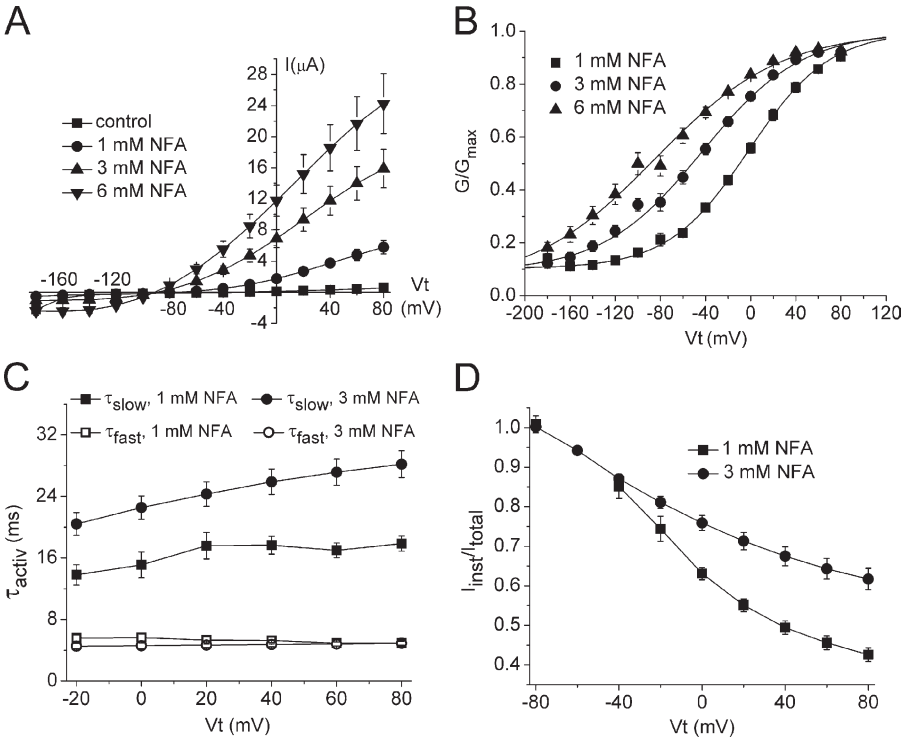

Figure 5. Concentration-dependent effects of NFA on $I_{Slo2.1}$ magnitude and kinetics. (A) I-V relationships determined before (control) and after treatment of oocytes with 1, 3, and 6 mM NFA as indicated. (B) G-V relationships based on I-V relationships plotted in A. Data were fitted with a Boltzmann function (smooth curves) to determine the half-point ($V_{1/2}$) and effective valence, z, for $I_{Slo2.1}$ activated by treatment of oocytes with NFA. The $V_{1/2}$ was -1 ± 0.7 mV ($n = 8$), -43 ± 2.4 mV ($n = 7$), and -84 ± 6 mV ($n = 5$) for 1, 3, and 6 mM NFA, respectively. The z values were 0.71 ± 0.01, 0.57 ± 0.02, and 0.46 ± 0.02 for oocytes treated with 1, 3, and 6 mM NFA, respectively. (C) Kinetics of $I_{Slo2.1}$ activated by NFA. A summary of the fast and slow time constants (τfast and τslow) for activation of the time-dependent component of current ($n = 15$ for 1 mM NFA and $n = 14$ for 3 mM NFA). (D) A plot of the amplitude of the instantaneous current (I_{inst}) divided by total outward current (I_{total}) as a function of text potential, V_t ($n = 14$–15).

more positive. For V_t of +80 mV, I_{inst}/I_{total} was 0.42 with 1 mM NFA and 0.62 with 3 mM NFA (Fig. 5 D).

Voltage dependence of Slo2.1 activation is modulated by $[K^+]_o$

The effect of $[K^+]_e$ on NFA-activated $I_{Slo2.1}$ was determined. For these experiments, $[K^+]_e$ was varied from 1 to 99 mM, and the sum of $[K^+]_e + [Na^+]_e$ was maintained at 100 mM. The I-V relationships were first determined for $[K^+]_e$ = 1 mM and $[Na^+]_e$ = 99 mM. The $[K^+]_e$ was then sequentially elevated to 3, 10, 30, and 99 mM (with appropriate reduction in $[Na^+]_e$), and the I-V relationships were determined after equilibration in each solution. For these experiments, 1 mM NFA was used. In another batch of oocytes, the I-V relationships were also determined in a solution containing 300 mM KCl. For these oocytes, currents were first measured in a solution containing 99 mM KCl before switching to the 300-mM KCl solution, and recordings were made 2 min after the change in resting potential reached an equilibrium and before the hypertonic solutions caused significant cell shrinkage. Elevation of $[K^+]_e$ caused a rightward shift of the I-V relationships (Fig. 6 A), but the slope conductance of outward currents was not altered at equivalent

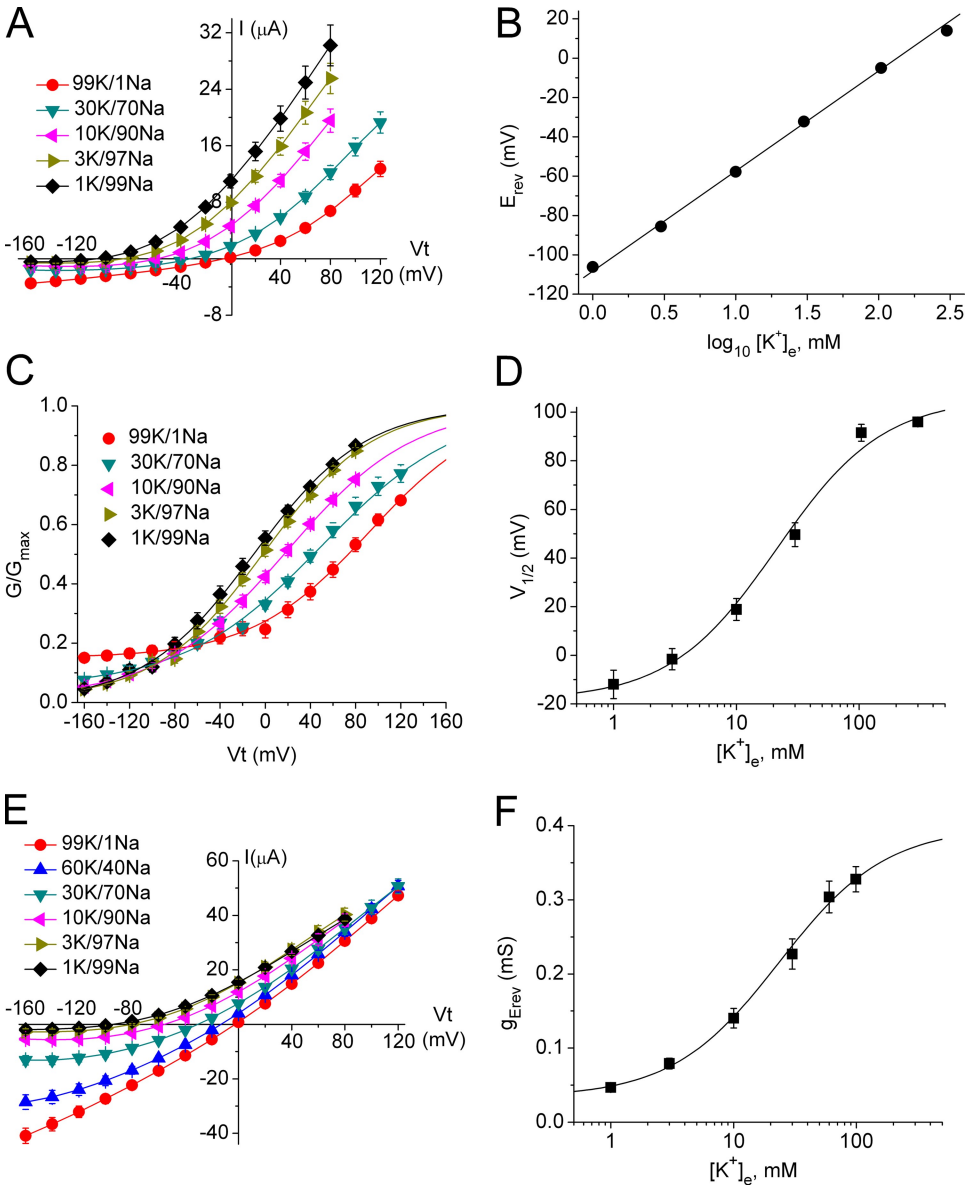

Figure 6. Voltage dependence of Slo2.1 channel activation is $[K^+]_e$ dependent. (A) I-V relationships for $I_{Slo2.1}$ activated with 1 mM NFA in oocytes bathed in an extracellular solution, where $[K^+]_e$ was varied from 1 to 99 mM. $[Na^+]_e$ was varied as indicated, so that the sum of $[K^+]_e$ and $[Na^+]_e$ was kept constant at 100 mM. Currents were measured from oocytes (n = 5) 3 d after they were injected with 0.84 ng cRNA. (B) Slo2.1 is K^+ selective. Reversal potential of $I_{Slo2.1}$ (E_{rev}) was plotted as a function of $\log_{10}[K^+]_e$, and the data were fitted by linear regression. The slope of the line is 50.5 mV/decade increment of $[K^+]_e$ (R^2 = 0.99). (C) G-V relationships for Slo2.1 as a function of $[K^+]_e$. (D) $V_{1/2}$ of G-V relationship plotted as a function of $\log_{10}[K^+]_e$. The data were fitted with a Hill equation (smooth curve) with an EC_{50} of 21.2 ± 6.0 mM when the Hill coefficient, n_H, was fixed to a value of 1.0 (R^2 = 0.99). The data for 300 mM $[K^+]_e$ was measured in a separate batch of oocytes. (E) I-V relationships for $I_{Slo2.1}$ activated with 3 mM NFA in oocytes bathed in an extracellular solution, where $[K^+]_e$ was varied from 1 to 99 mM. $[Na^+]_e$ was varied as indicated, so that the sum of $[K^+]_e$ and $[Na^+]_e$ was kept constant at 100 mM. Currents were measured from oocytes (n = 6) 2 d after they were injected with 0.84 ng cRNA. (F) The slope conductance was determined at the 0 current potential (g_{Erev}) of the I-V relationship and plotted as a function of $\log_{10}[K^+]_e$. The data were fitted with a Hill equation (smooth curve) with an EC_{50} of 23.5 ± 3.5 mM when the Hill coefficient, n_H, was fixed to a value of 1.0 (R^2 = 0.99).

values of $V_t - E_{rev}$. As expected for a K^+-selective channel, E_{rev} varied as a linear function of $\log_{10}[K^+]_e$ (Fig. 6 B), with a slope (50.5 mV/decade) that was close to value (56 mV/decade) predicted by the Nernst equation. The G-V relationships derived from the I-V relationships are plotted in Fig. 6 C. The $V_{1/2}$ for activation was shifted to more positive potentials as $[K^+]_e$ was increased from 1 to 300 mM, with an EC_{50} of 21.2 ± 6.0 mM (Fig. 6 D). We next used a higher concentration of NFA (3 mM) to further activate channels and facilitate the measurement of the slope conductance at E_{rev} (g_{Erev}) as a function of $[K^+]_e$ that was varied from 1 to 99 mM. The I-V relationship for currents measured in five oocytes is summarized in Fig. 6 E. Similar to the shift in $V_{1/2}$ of the G-V relationship, g_{Erev} was increased as a sigmoidal function of $\log_{10}[K^+]_e$, with an EC_{50} of 23.5 ± 3.5 mM.

Outward rectification of the $I_{Slo2.1}$-V_t relationships results from the combined effects of voltage-dependent channel gating and the decrease in single-channel current magnitude at negative potentials predicted by the Goldman-Hodgkin-Katz (GHK) current equation (Goldman, 1943; Hodgkin and Katz, 1949). The GHK component dominates for large transmembrane gradients of K^+, but is negligible for a $[K^+]_e$ of 99 mM, assuming a $[K^+]_i$ of 110 mM in oocytes (Weber, 1999). In Fig. 7, the normalized I-V and G-V relationships for $I_{Slo2.1}$ measured in oocytes bathed in an extracellular solution containing 2, 10, or 99 mM KCl are plotted (filled squares and filled curves) and compared with the relative current magnitude and corresponding "G-V" relationships predicted by the GHK current equation (dashed curves). This comparison clearly shows that outward rectification of the I-V relationships determined with a $[K^+]_e$ of 2 or 10 mM is mainly a consequence of the asymmetrical transmembrane gradient in $[K^+]$. However, the inward currents measured at $V_t < -120$ mV are significantly smaller that the GHK-predicted values. Moreover, unlike the experimental data summarized in Fig. 6 C, the $V_{1/2}$ of the GHK-predicted G-V relationships do not shift as a function of $[K^+]_e$. An excised, inside-out patch containing a single Slo2.1 channel also exhibited reduced inward currents compared with the level predicted by the GHK current equation (Fig. 8). A single current trace recorded during a voltage ramp from +80 to −120 mV is shown in Fig. 8 A. For this experiment, $[K^+]_e$ was 10 mM and $[K^+]_i$ was 90 mM. In Fig. 8 B, the ensemble averaged current from 37 voltage ramps is compared with the i-V relationship predicted by GHK for a voltage-independent K^+-selective channel. Collectively, these findings indicate that the weak voltage dependence of Slo2.1 measured under asymmetrical K^+ conditions is at least partially due to channel gating (reduced P_o) and not simply caused by a reduced single-channel conductance. Under nearly symmetrical $[K^+]$ conditions (99 mM K^+ outside and 110 mM K^+ inside), the whole cell I-V relationship is predicted to be a nearly linear function of voltage, yet

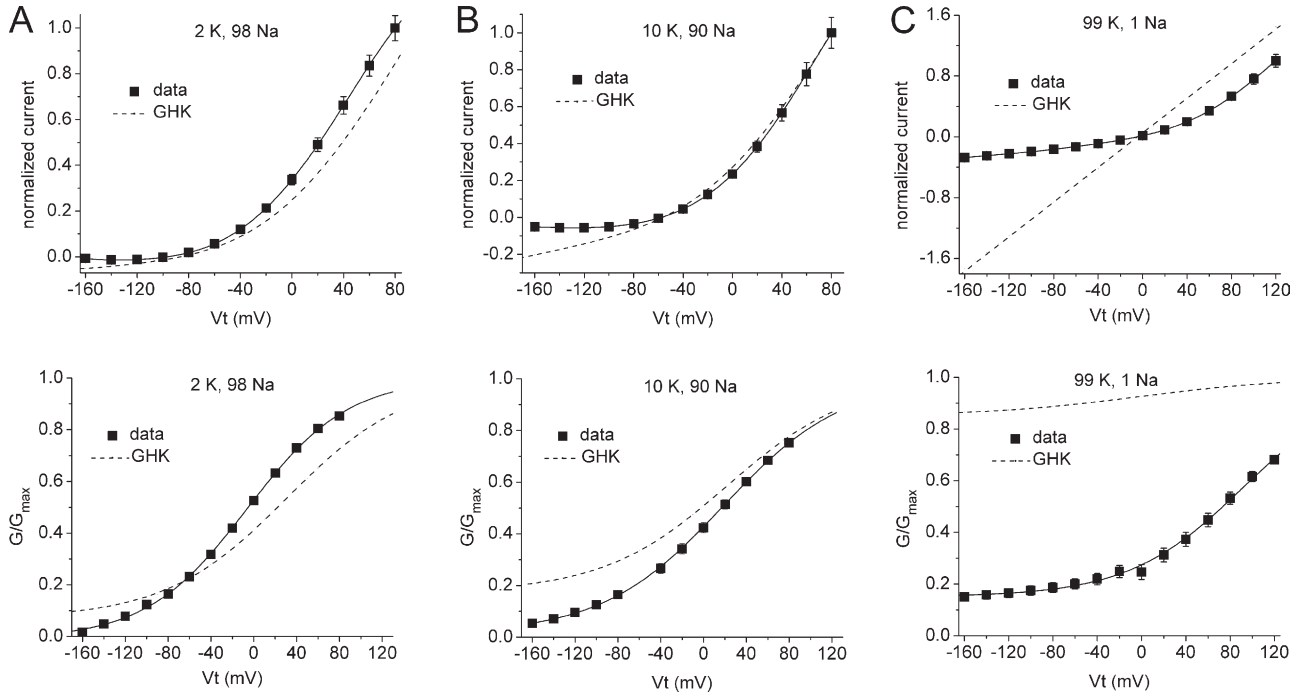

Figure 7. I-V and G-V relationships measured from oocytes compared with relationships predicted by GHK current equation. (A) I-V relationships (top) and G-V relationships determined for $[K^+]_e$ = 2 mM. (B) Relationships determined for $[K^+]_e$ = 10 mM. (C) Relationships determined for $[K^+]_e$ = 99 mM.

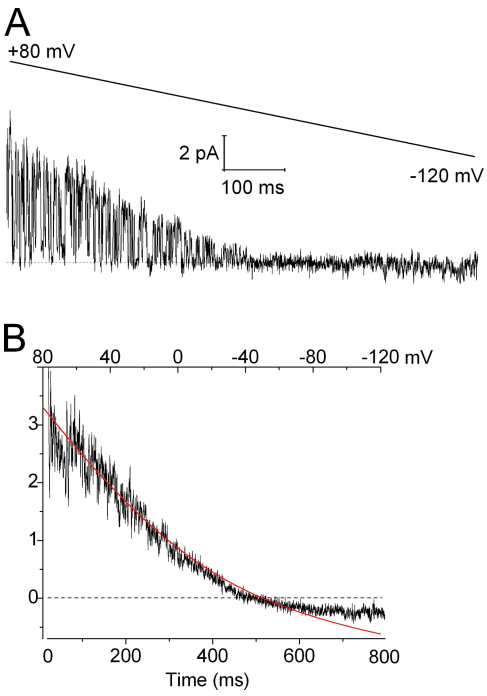

Figure 8. Slo2.1 channel rectification is greater than that predicted by GHK current equation. (A) Single Slo2.1 channel activity measured in an excised inside-out patch during a voltage ramp as indicated. Extracellular (pipette) solution contained (in mM): 90 NaCl, 10 KCl, 0.1 $CaCl_2$, 2 $MgCl_2$, 10 HEPES, and 1 NFA, pH 7.2; intracellular (bath) solution contained (in mM): 90 KCl, 10 NaCl, 2 EGTA, 10 HEPES, and 2 $MgCl_2$, pH 7.2. The holding potential was −80 mV, and the voltage was stepped to +80 mV, and then ramped down to −120 mV over 775 ms. The slope conductance for this single channel at positive potentials was 55 pS. (B) Ensemble average currents recorded during 37 voltage ramps. The red curve represents the i-V relationship predicted by the GHK current equation for a voltage-independent conductance.

the measured $I_{Slo2.1}$-V_t relation showed a prominent outward rectification in cells treated with 1 mM NFA (Fig. 7 C).

Voltage dependence of Slo2.1 channel activation is altered by NFA

As shown in Fig. 6, in addition to enhancing the magnitude of $I_{Slo2.1}$, increasing [NFA] from 1 to 3 mM also reduced the extent of outward rectification of the I-V relationship. We quantified this effect more completely by treatment of oocytes with 1–6 mM NFA, a concentration range that induced current increases equivalent to a 20–90% of the maximal response (Fig. 2 D). The extracellular solution contained 104 mM KCl and 0 mM NaCl (K104), and currents were recorded during test pulses applied to voltages ranging from −160 to +120 mV. The holding potential was 0 mV, and a 100-ms prepulse to −80 mV was applied. Two groups of oocytes were evaluated, treated with either 1–3 mM NFA or 4–6 mM NFA. The average I-V relationships measured in these oocytes are plotted in Fig. 9 (A and B, respectively). Outward rectification was reduced by NFA in a concentration-dependent manner. The corresponding G-V relationships are plotted in Fig. 9 C. The $V_{1/2}$ for activation was shifted in a [NFA]-dependent manner, with an EC_{50} of 2.1 ± 0.2 mM (n_H = 2.9 ± 0.1). In addition, the minimum value of G/G_{max} was increased as a function of [NFA] (Fig. 9 D), with an EC_{50} of 2.4 ± 0.2 mM (n_H = 1.9 ± 0.3).

The results described above for whole cell currents were confirmed in single-channel recordings from inside-out patches. From a holding potential of −80 mV, a 1-s voltage ramp was applied from +80 to −120 mV. When the pipette contained 1 mM NFA, the P_o of the single channel in the patch was high at positive potentials and low at negative potentials (Fig. 10 A, *i–iii*), resulting in outward rectification of the ensemble averaged i-V relationship (Fig. 10 A, *iv*). In contrast, when the pipette contained 6 mM NFA, channel activity remained nearly constant throughout the voltage ramp (Fig. 10 B, *i–iii*), and the ensemble averaged i-V relationship was linear (Fig. 10 B, *iv*). The i-V relationship for single channels exhibited inward rectification in the presence of NFA (Fig. 10 C).

The conductance of Slo2.1 is modulated by extracellular monovalent cations

Outward rectification of $I_{Slo2.1}$ in the presence of high $[K^+]_e$ could result from the removal of a blocking effect by extracellular Na^+ ions. To test this possibility, we replaced the 96-mM NaCl in the extracellular solution with enough mannitol to maintain a constant osmolarity. Substitution of NaCl with mannitol reduced Slo2.1 current by ∼65% (Fig. 11 A). Na^+ was also replaced with Rb^+ (a permeable cation), Li^+ and Cs^+ (nonpermeable cations similar in size to Na^+), or choline (a large, nonpermeant cation). Monovalent cations have variable effects on Na^+ pump activity (Robinson, 1975; Akera et al., 1979) and would therefore cause differential changes in $[Na^+]_i$. Therefore, all oocytes for these experiments were pretreated for 10 min with 10 μM ouabain before switching to the Na^+-free extracellular solutions. The I-V relationships for WT Slo2.1 channels were recorded in oocytes bathed in standard KCM411 solution and in KCM411 with Na^+ replaced with the cation as indicated in Fig. 11. Choline reduced outward $I_{Slo2.1}$ by ∼55% (Fig. 11 B), similar to the effect of mannitol. Li^+ did not alter currents (Fig. 11 C). Cs^+ blocked inward currents, but did not significantly affect the magnitude of steady-state outward currents (Fig. 11 D). The permeant cation Rb^+ (Fig. 11 E) did not affect outward conductance when corrected for the change in driving force ($V_t - E_{rev}$), and the slope conductance of inward currents was increased as predicted by the GHK current equation. Finally, the dependence of slope conductance on $[Na^+]_e$ was determined. Oocytes were bathed in an extracellular solution containing 3 mM NFA and a $[K^+]_e$ of 10 mM; $[Na^+]_e$ was varied from 0 to 90 mM by isoosmolar substitution with mannitol

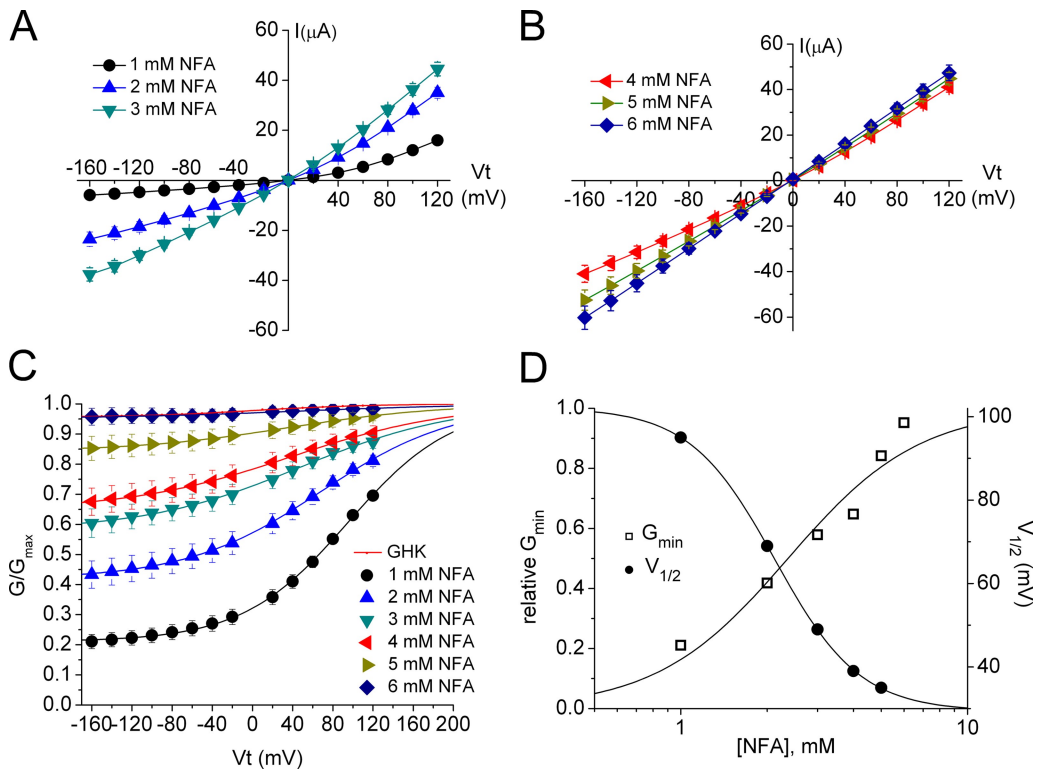

Figure 9. NFA decreases rectification of $I_{Slo2.1}$. (A) Average $I_{Slo2.1}$-V relationships in oocytes treated sequentially with 1, 2, and 3 mM NFA ($n = 8$). (B) Average $I_{Slo2.1}$-V relationships in another batch of oocytes treated sequentially with 4, 5, and 6 mM NFA ($n = 6$). Extracellular solution was K104. (C) G-V relationships for $I_{Slo2.1}$ for different concentrations of NFA as indicated. (D) Shift in $V_{1/2}$ of the G-V relationship (filled circles) and minimum value of G/G_{max} (open squares) is [NFA] dependent. Data were fitted with a Hill equation (smooth curves). For shift in $V_{1/2}$, EC_{50} = 2.1 ± 0.2 mM and n_H = 2.9 ± 0.1 (R^2 = 1.0). For minimum G/G_{max}, EC_{50} = 2.4 ± 0.2 mM and n_H = 1.9 ± 0.3 (R^2 = 0.93).

(Fig. 11 F). A plot of maximum slope conductance (from linear fit to currents measured between +40 and +80 mV) versus $[Na^+]_e$ was fitted with a Hill equation (Fig. 11 F, inset) to obtain an EC_{50} for $[Na^+]_e$ of 10.5 mM and a Hill coefficient of 0.72. Thus, normal conductance of Slo2.1 channels requires the presence of physiological levels of extracellular monovalent cations, either Na^+ or other small permeant cations (K^+ or Rb^+) or nonpermeant cations (e.g., Li^+).

Mutation of charged residues located in the S1–S4 segments of Slo2.1 do not induce large changes in the voltage dependence of channel activation

Consistent with its weak voltage dependence of activation, the S4 domain of Slo2.1 contains an unusually low number of charged residues. In fact, the S4 of Slo2.1 has two basic and two acidic residues, a net charge of 0. In contrast, Slo1 and Shaker have three and seven basic residues, respectively, in their S4 domains (Fig. 12 A). The functional voltage sensor of the related Slo1 channel is proposed to be composed of four charged residues: one in S4, two in S2, and one in S3 (Ma et al., 2006). Slo2.1 also has several charged residues in the S1, S2, and S3 domains (Fig. 12 B). To determine if any of the charged residues in the S1–S4 segments of Slo2.1 contribute to voltage sensing, the acidic and basic residues in this region were neutralized by mutation to Ala. K70 and R80 of the S1 segment were individually mutated, whereas mutations of E118 in S2 and E143 in S3 were combined into a single mutant channel construct. Similar to WT Slo2.1, currents were not detectable in oocytes injected with cRNA for these mutant channels in response to test potentials ranging from −160 to +120 mV when oocytes were bathed in K104 solution. However, robust outwardly rectifying currents were elicited by treatment of these oocytes with 1 mM NFA (Fig. 13, A–C). The G-V relationships for K70A, R80A, and E118A/E143A Slo2.1 channels were similar to WT channels (Fig. 13 D). Mutations of the four charged residues (K174, E178, D183, and R186) and two His residues (H175 and H185) of the S4 segment were combined into a single mutant channel. The I-V relationship for this "S4 neutral" channel rectified normally (Fig. 13 E), and the G-V relationship was also similar to WT channels (Fig. 13 F). The rectification of the I-V relationships for WT and the S1–S4 mutant channels is best compared when currents were normalized to their maximum values measured at +120 mV (Fig. 13 G). This plot reveals that the outward rectification of all the mutant channels is similar to WT channels and very

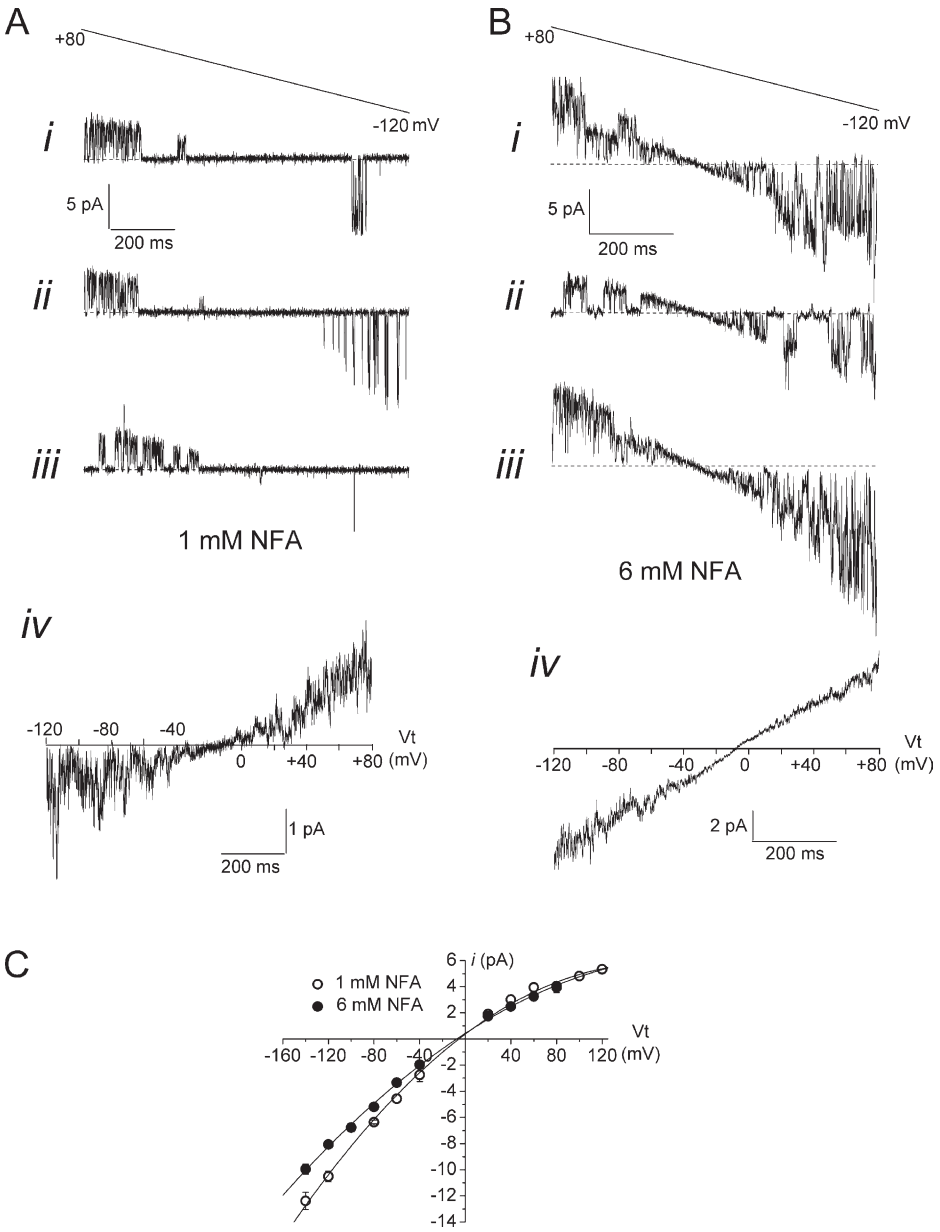

Figure 10. The effect of 1 and 6 mM NFA on single Slo2.1 channel activity. (A) Activity of a single Slo2.1 channel in an inside-out patch activated with 1 mM NFA in the pipette solution and recorded during voltage ramps from +80 to −120 mV. For these experiments, the extracellular (pipette) solution contained (in mM): 99 K gluconate, 1 Na gluconate, 2 $MgCl_2$, 0.1 $CaCl_2$, 0.1 $GdCl_3$, 10 HEPES, and either 1 or 6 NFA. The intracellular (cell chamber) solution was the same, except that $CaCl_2$ was replaced with 2 mM EGTA, and NFA was not present. Three different current traces (*i–iii*) are shown together with the ensemble average of 15 traces (*iv*) plotted on a reversed voltage scale. Note outward rectification of currents. (B) A different inside-out patch showing activity of at least two channels that were activated by 6 mM NFA in the pipette solution. Three different current traces (*i–iii*) are shown together with the ensemble average of 30 traces (*iv*) plotted on a reversed voltage scale. Note that currents do not exhibit rectification. (C) i-V relationships for single Slo2.1 channels activated by 1 mM (n = 3) or 6 mM (n = 6) NFA. The slope conductance determined from channels activated between −60 and −140 mV was 97 ± 11 pS for 1 mM NFA (n = 3) and 80 ± 2 pS for 6 mM NFA (n = 5).

unlike the near-linear relationship expected for a voltage-independent channel, calculated according to the GHK current equation and shown in this graph as a dotted line. Collectively, these findings indicate that charged residues in the S1–S4 domains are not important for voltage sensing, and that the weak voltage dependence of Slo2.1 channel activation is not mediated by the structural equivalent of the VSD in Kv channels.

Mutation of R190 uncouples Slo2.1 channel activation from obligate dependence on elevated $[Na^+]_i$ or NFA

Sequence alignment of Slo2.1 with Kv channels suggests that R190 is located either at the C terminus of the S4 segment or at the beginning of the intracellular S4–S5 linker (Fig. 12). Unlike mutations in S1–S4, mutation of R190 to Ala or Gln produced channels that were active in the absence of NFA. Treatment with 1 mM NFA only modestly enhanced the magnitude of R190A $I_{Slo2.1}$ (Fig. 14, A and B) and increased R190Q $I_{Slo2.1}$ by approximately twofold (Fig. 14, C and D). The basal activity of R190A and R190Q channels explains the reduction of the extent of activation by NFA (compared with WT channels). Mutation of R190 to another basic residue (R190K) produced channels with properties that resembled WT channels with respect to basal current (barely detectable) and sensitivity to 1 mM NFA (∼15-fold increase in current magnitude; Fig. 14, E and F). To further examine the importance of a basic residue, R190 was mutated to an acidic residue (Glu). Injection of oocytes with 0.84 ng R190E Slo2.1 cRNA induced large, time-independent $I_{Slo2.1}$ under control conditions, and unlike WT, R190A, or R190Q channels, whole cell

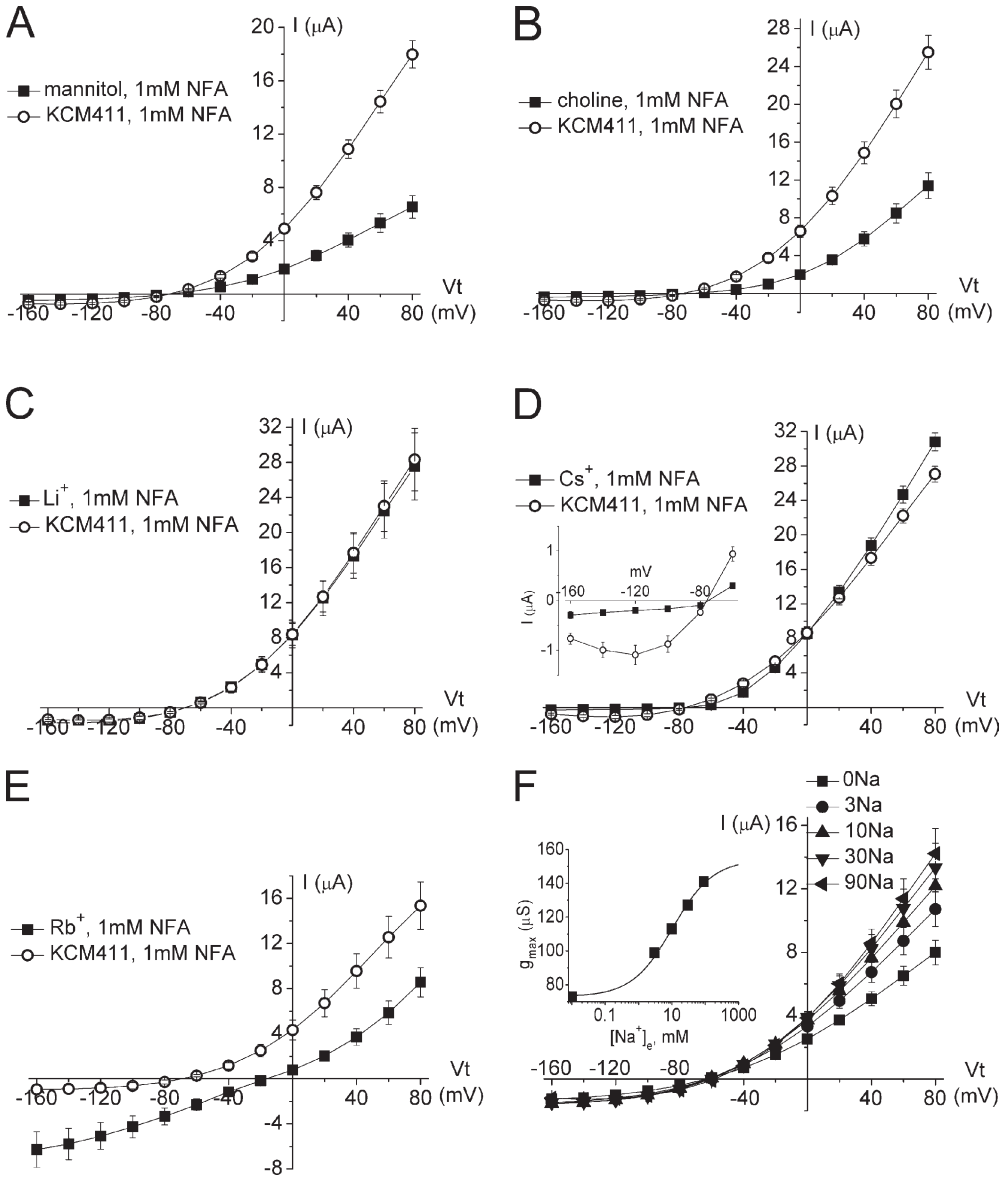

Figure 11. Effects of replacing extracellular Na^+ with mannitol, choline, or monovalent cations on Slo2.1 channel currents. (A–E) $I_{Slo2.1}$-V relationships for oocytes bathed in KCM411 extracellular solution and activated by 1 mM NFA before and after replacement of extracellular Na^+ with either mannitol or indicated monovalent cation. (A and B) Currents recorded from oocytes 3 d after injection with 0.32 ng cRNA ($n = 6$). (C and D) Currents recorded from oocytes 3 d after injection with 0.84 ng cRNA (n = 5–6). (D, inset) Currents for V_t of −60 to −160 mV at an expanded scale. (F) $I_{Slo2.1}$–V relationships for oocytes activated by 3 mM NFA and bathed in an extracellular solution containing the indicated level (in mM) of NaCl. $[Na^+]_e$ was varied from 0 to 90 mM by substitution with mannitol to maintain constant osmolarity ($n = 6$). Currents were recorded 3 d after injection of oocytes with 0.32 ng cRNA. Inset shows plot of maximum slope conductance as a function of $\log_{10}[Na^+]_e$. Data were fitted to a Hill equation (smooth curve; $EC_{50} = 10.5 \pm 4.2$ mM, $n_H = 0.72 \pm 0.13$, and $R^2 = 0.997$).

currents were not further activated by treatment of oocytes with 1 mM NFA (Fig. 14, G and H). Collectively, these findings indicate that a basic residue at position 190 in Slo2.1 is required for normal channel gating, and that neutralization or charge reversal of R190 induces constitutive channel activation or enhances the sensitivity of the channels to $[Na^+]_i$. We tested for the latter possibility by determining the effects of Na_i loading on oocytes expressing R190E channels (Fig. 15 A). Currents were recorded in cells bathed first in KCM211 and then in K104 solution. Channels were constitutively active regardless of $[K^+]_e$. The cells were then incubated in Na_i-loading solution for 15 min, and the I-V relationships were again determined. Currents were increased by Na_i loading with K104, but not with KCM211 extracellular solution. In another batch of oocytes, we determined the effects of 1 mM NFA on R190E Slo2.1 channel activity. NFA induced a modest increase in the magnitude of outward $I_{Slo2.1}$, but more than doubled inward currents (Fig. 15 B), eliminating outward rectification of the I-V relationship (Fig. 15 C). Thus, R190E channels are constitutively open and not simply more responsive to intracellular Na^+ when oocytes are bathed in a low K^+ extracellular solution. In contrast, when oocytes were bathed in a high K^+ extracellular solution, R190E channels had a reduced level of constitutive activity and therefore could be activated by elevated $[Na^+]_i$ or administration of extracellular NFA. The $[K^+]_e$ dependence of constitutive Slo2.1 channel activity was more exaggerated for R190A and R190Q channels. The currents recorded in oocytes expressing R190A Slo2.1 channels were only slightly larger than the endogenous currents of uninjected oocytes bathed in K104 solution, but exposure to 1 mM NFA induced a robust increase in currents that did not exhibit rectification (Fig. 15 D). The same low level of constitutive activity and robust

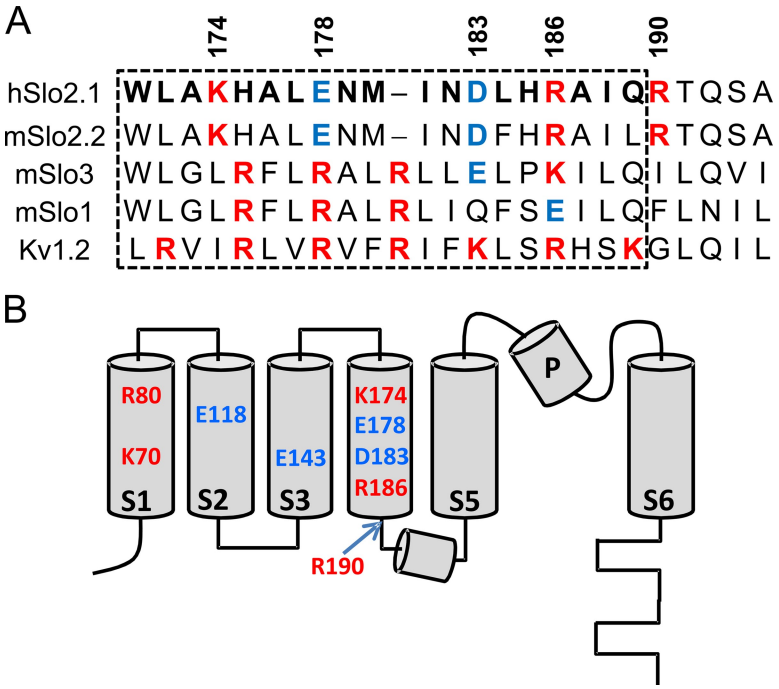

Figure 12. Location of charged residues in the S1–S4 segments of Slo2.1 channel subunits. (A) Sequence alignment of S4 segments for Slo and Kv1.2 channels. Numbering on top refers to residues in hSlo2.1, and box indicates the boundaries of the S4 segment. Basic residues are colored red, and acidic residues are colored blue. (B) Diagram of a single Slo2.1 subunit showing location of charged amino acids in the S1–S4 segments.

response to 1 mM NFA was observed for R190Q channels (Fig. 15 E). Finally, we determined the concentration-dependent effects of NFA on WT, R190A, and R190E channel currents measured in oocytes bathed in KCM211 and K104 solution. The I-V relationships for R190A and R190E channels determined using KCM104 solutions are presented in Fig. 16 (A and B). The maximum response to NFA was much greater for R190A than R190E channels. This is seen more clearly in Fig. 16 C, where the [NFA]–response relationships are plotted for currents measured at +80 mV. For comparison, the [NFA]–response relationships for oocytes bathed in low K^+ (KCM211) solution are plotted in Fig. 16 D. Although the potency of NFA was greater for R190A and R190E compared with WT $I_{Slo2.1}$, the efficacy (increase over basal level) was diminished by these mutations. For example, in the presence of low external $[K^+]_e$ (Fig. 16 D), the EC_{50} for R190A $I_{Slo2.1}$ was 0.7 mM compared with 2.1 mM for WT $I_{Slo2.1}$. This was associated with a maximum increase in R190A $I_{Slo2.1}$ of five-fold compared with an 80-fold increase for WT $I_{Slo2.1}$. The slight (~15%) increase in currents induced by high concentrations of NFA in oocytes expressing R190E channels can be accounted for by the activation of endogenous K_{Na} channels. Collectively, these findings indicate that the constitutive activity of R190 mutant Slo2.1 channels is dependent on $[K^+]_e$, and that when $[K^+]_e$ is low, R190E are fully activated; i.e., they are not further activated by treatment with NFA or elevation of $[Na^+]_i$.

DISCUSSION

Under normal physiological conditions, K_{Na} channels are in a nonconducting state and are only activated by a significant elevation of $[Na^+]_i$ (Dryer, 1994). Although elevation of $[Na^+]_i$ during the upstroke of a single neuronal action potential may not be sufficient to activate K_{Na} channels (Dryer, 1991), these channels can be induced to open after a rapid train of action potentials (Safronov and Vogel, 1996). Inhibition of the Na^+ pump by ischemia or cardiac glycosides can also activate K_{Na} in cardiac myocytes (Luk and Carmeliet, 1990). As reported here, cloned Slo2.1 channels expressed in *Xenopus* oocytes have a very low P_o until activated by inhibiting the Na^+ pump with a K^+-free solution or ouabain. Although these are simple methods to activate channels in oocytes, the final level of $[Na^+]_i$ achieved is uncertain and not easily controlled when measuring whole cell currents. Excised patch recording of single- or multiple-channel activity with discrete changes in $[Na^+]_i$ is obviously a more quantitative approach for characterization of Slo2.1 properties, but this approach suffers from the possibility that unknown intracellular diffusible cofactors that alter channel gating or sensitivity to $[Na^+]_i$ are lost upon patch excision. For example, NAD^+ was recently reported to decrease the EC_{50} for intracellular Na^+ from 50 to 20 mM in DRG neurons and heterologously expressed Slo2.2 channels (Tamsett et al., 2009).

Based on previous reports that NFA activates large-conductance Ca^{2+}-activated K^+ (Slo1) channels (Ottolia and Toro, 1994; Greenwood and Large, 1995; Gribkoff et al., 1996), we reasoned that this compound or other fenamates might also activate Slo2.1. These compounds proved to be more effective than anticipated and facilitated the measurement of robust currents in oocytes injected with as little as 0.2 ng cRNA. For comparison, 75 ng

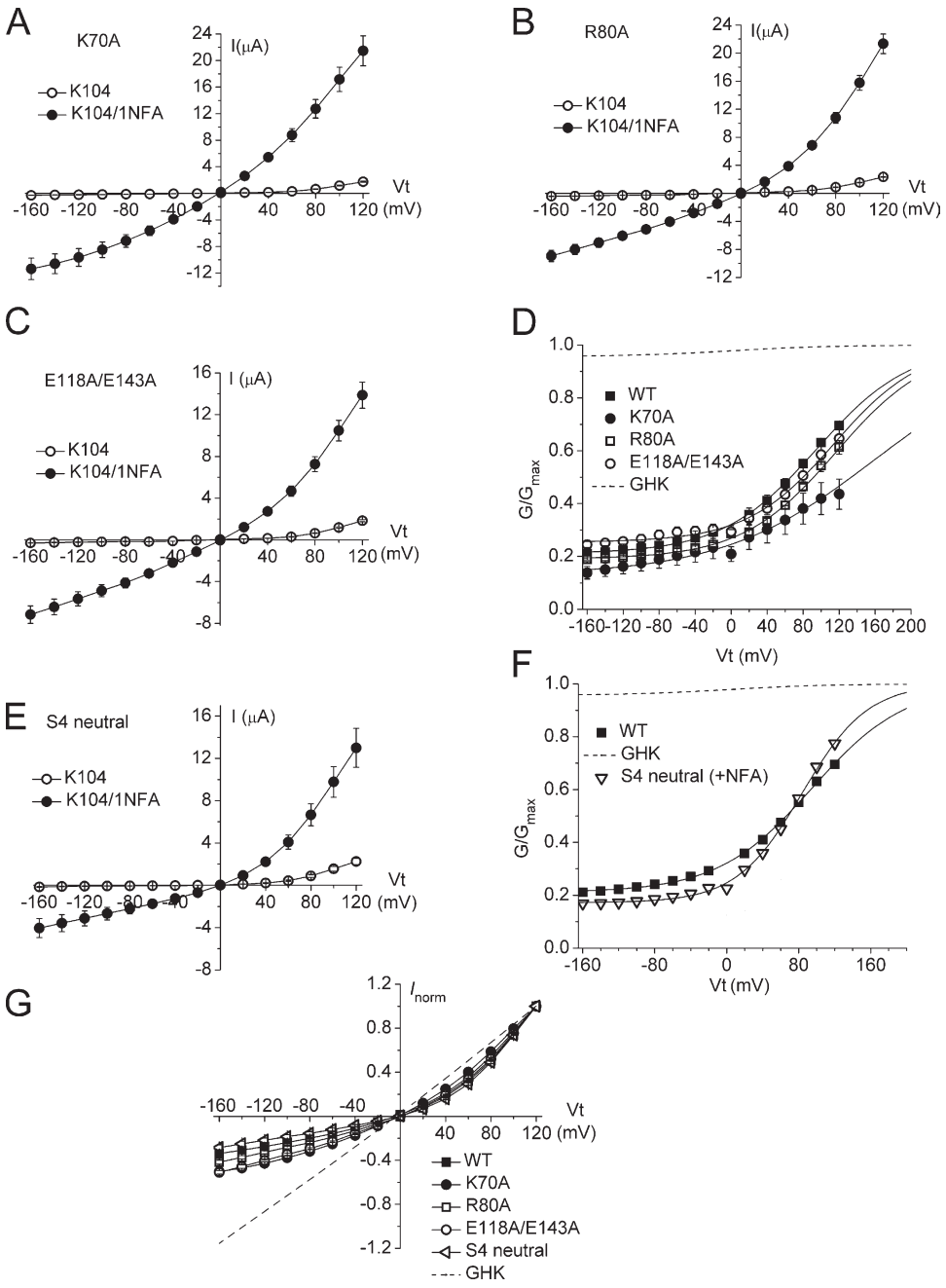

Figure 13. Neutralization of charged residues in the S1–S4 segment does not eliminate voltage-dependent gating of Slo2.1 channels. (A and B) I-V relationships for currents recorded from oocytes expressing S1 mutant K70A Slo2.1 (n = 14) or R80A Slo2.1 (n = 7) channels before and after treatment with 1 mM NFA. Extracellular solution was K104. Oocytes were recorded 2 d after injection of 2.5 ng cRNA. (C) I-V relationships for currents recorded from oocytes expressing the S2 double mutant (E118A/E143A) Slo2.1 channels before and after treatment with 1 mM NFA (n = 7). Oocytes were recorded 2 d after injection of 2.5 ng cRNA. (D) G-V relationships for WT and S1–S3 mutant channels. Dotted curve shows relationship predicted by GHK current equation for voltage-independent channel. The data were fitted with a Boltzmann function (smooth curves) to obtain $V_{1/2}$ and z values as follows. WT: $V_{1/2}$ = +95 ± 0.6 mV and z = 0.48 ± 0.01; K70A: $V_{1/2}$ = +159 ± 8 mV and z = 0.30 ± 0.04; R80A: $V_{1/2}$ = +116 ± 3 mV and z = 0.48 ± 0.02; E118A/E143A: $V_{1/2}$ = +114 ± 4 mV and z = 0.51 ± 0.04. (E) I-V relationships for currents recorded from oocytes expressing the S4 neutral mutant (K174A/E178A/D183A/R186A/H175A/H185A) Slo2.1 channels before and after treatment with 1 mM NFA (n = 9). Oocytes were recorded 3 d after injection of 9.2 ng cRNA. (F) G-V relationships for WT and S4 neutral mutant channels (+84 ± 1 mV; z = 0.69 ± 0.02). Dotted curve shows relationship predicted by GHK current equation for voltage-independent channel. (G) Normalized I-V relationships for WT and S1–S4 mutant channels. Currents for each channel type were normalized to their average values measured at +120 mV.

cRNA per oocyte was used in previous studies of Slo2.1 (Santi et al., 2006). The [NFA]–response relationship had a Hill coefficient of 1.9, indicating a positively cooperative reaction and the possibility that two NFA molecules can bind to each Slo2.1 channel. The molecular basis of NFA activation of Slo2.1 or other K^+ channels is unknown, but in all cases, the compound acts extremely fast after application. Moreover, NFA preferentially increases P_o of BK (Slo1) channels reconstituted in bilayers when applied from the external side of the channel (Ottolia and Toro, 1994). Thus, the binding site for NFA on Slo1 and Slo2.1 channels is most likely located within a region of the protein that is readily accessible from the extracellular solution. Although much remains to be discovered regarding the mechanisms of channel activation by fenamates, treatment of cells with

these compounds represents a simple technique to activate whole cell Slo2.1 currents.

Outward rectification of $I_{Slo2.1}$ measured in the presence of low $[K^+]_e$ can largely be accounted for by a reduced single-channel conductance at negative transmembrane potentials as predicted by the GHK current equation. However, outward rectification of the I-V relationship was still present in cells bathed in high K^+ solutions, despite an opposite-directed (inward) rectification of the single-channel i-V relationship. This indicates that variation in P_o of single channels accounts for the voltage dependence of the G-V relationship measured with high $[K^+]_e$ solutions. The very weak voltage dependence of Slo2.1 activation (z = 0.48 e when measured with 104 mM $[K^+]_e$) is more than 10 times less than a typical Kv channel, such as Shaker with a z of 6.8 e (McCormack et al., 1991). This difference is not unexpected given that the S4 domain of Slo2.1 has only two basic amino acids that are potentially offset by two acidic residues. By comparison, the S4 of Shaker has seven basic residues. Nonetheless, it is still possible that one or more of the charged residues in S4 or in the S1–S3 segments might contribute to the voltage dependence of Slo2.1 channel gating. A limited slope analysis of G-V

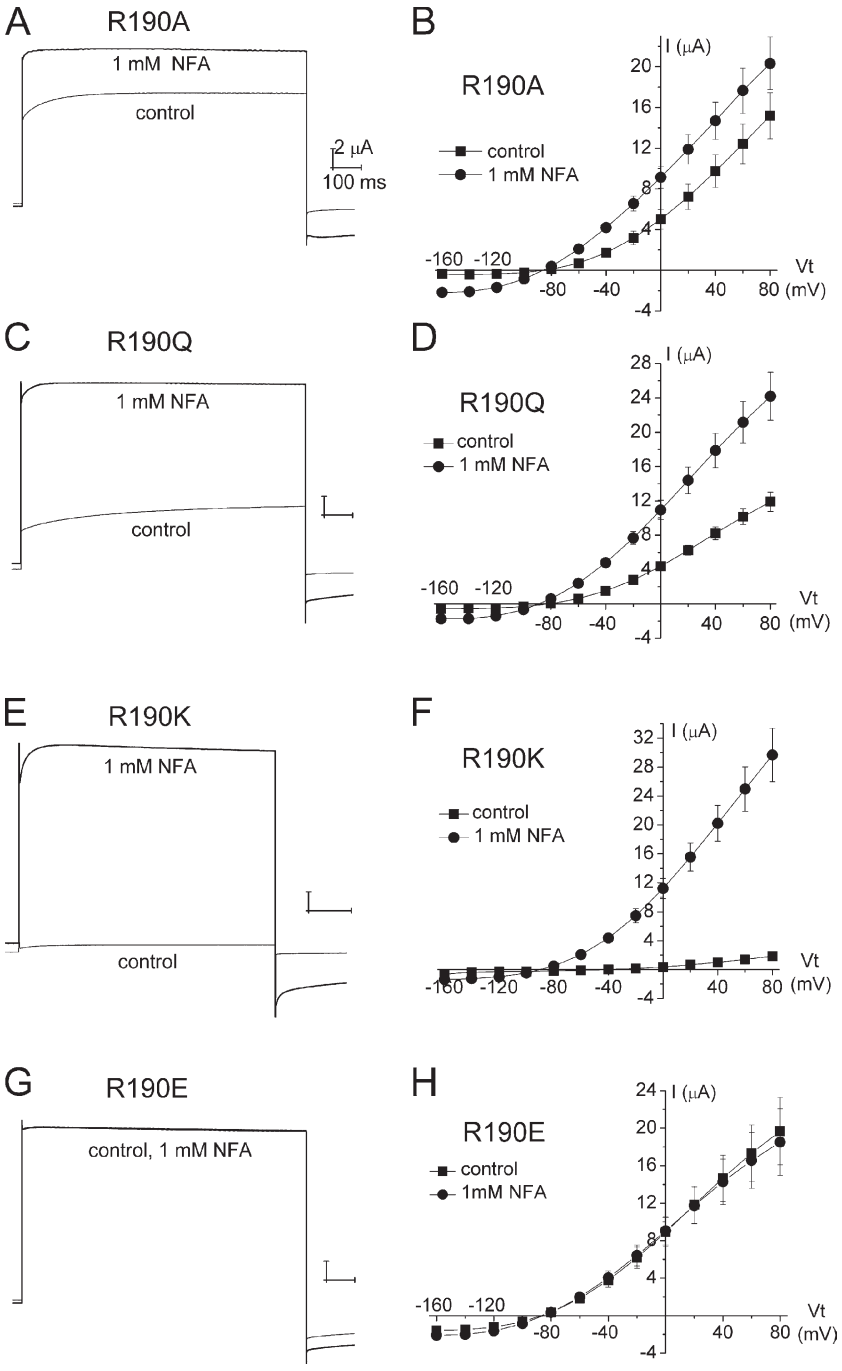

Figure 14. Nonconserved mutations of R190 in Slo2.1 induce constitutive channel activity and alter the sensitivity to NFA. (A) R190A current traces recorded at +40 mV before (control) and after treatment of oocytes with 1 mM NFA. (B) I-V relationships for R190A Slo2.1 channels determined in the presence and absence of 1 mM NFA (n = 5). Oocytes were recorded 2 d after injection of oocytes with 0.32 ng cRNA. (C) R190Q current traces recorded at +40 mV before (control) and after treatment of oocytes with 1 mM NFA. (D) I-V relationships for R190Q Slo2.1 channels determined in the presence and absence of 1 mM NFA (n = 8). Oocytes were recorded 2 d after injection of oocytes with 0.42 ng cRNA. (E) R190K Slo2.1 current traces recorded at +40 mV before (control) and after treatment of oocytes with 1 mM NFA. (F) I-V relationships for R190K Slo2.1 channels determined in the presence and absence of 1 mM NFA (n = 8). Oocytes were recorded 2 d after injection of oocytes with 0.84 ng cRNA. (G) 1 mM NFA does not activate R190E Slo2.1 currents recorded at +40 mV. Note that unlike the other R190 mutant channels, R190E channel currents are time independent in the absence of NFA. (H) NFA does not alter the I-V relationships for R190E Slo2.1 channels (n = 9). Oocytes were recorded 1 d after injection of oocytes with 0.84 ng cRNA.

curves may have revealed more subtle changes; however, as a first approximation, it is clear that mutation of charged residues in S1–S4 caused only minor changes in the voltage dependence of Slo2.1 activation. These findings indicate that the voltage dependence of activated Slo2.1 channel conductance is independent of the S1–S4 domains, the VSD of Kv channels.

Substitution of extracellular Na^+ with the large impermeant cation choline or mannitol (an uncharged sugar used to maintain osmolarity of extracellular solution) reduced outward currents, but did not increase the magnitude of inward currents. Thus, outward rectification of $I_{Slo2.1}$ measured with high $[K^+]_e$ solutions is not caused by block of inward currents by extracellular Na^+. Enhanced K^+ conductance in the presence of extracellular Na^+ was first reported for inward rectifier K^+ currents (Ohmori, 1978), where it was observed that replacement of extracellular Na^+ with choline, but not Li^+, reduced inward currents in tunicate eggs. The dependence of Slo2.1 channel conductance on $[Na^+]_e$ could conceivably be caused by changes in $[Na^+]_i$ or intracellular acidification subsequent to block of the Na^+/H^+ exchanger (Harvey and Ten Eick, 1989); however, this possibility was ruled out by our finding that replacement of Na^+ with equimolar Li^+ (which blocks the exchanger) did not alter g_{max}. The dependence of outward conductance on the presence of small extracellular cations, whether K^+, Rb^+, Na^+, or Li^+, suggests that these cations might increase channel P_o by binding to the outermost cation binding site (site 1) of the selectivity

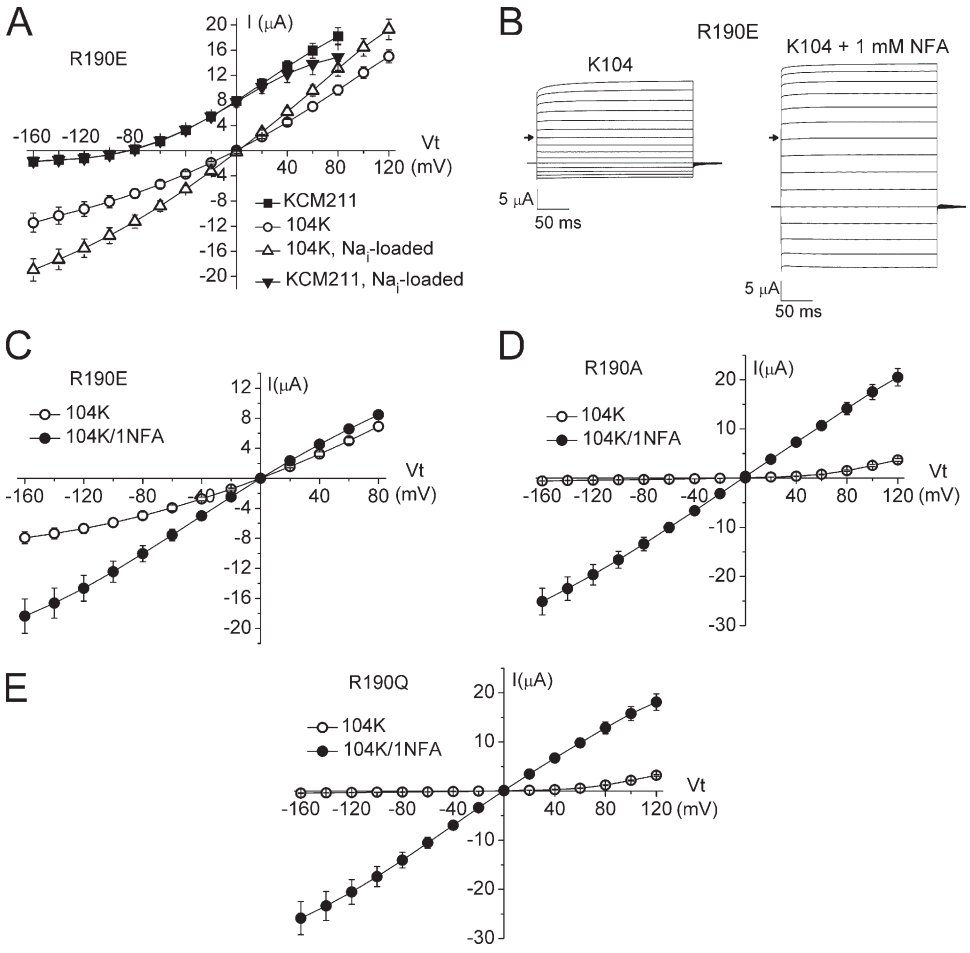

Figure 15. Activation of R190 mutant Slo2.1 channels by NFA or Na_i loading in oocytes bathed in high K^+ extracellular solution. (A) I-V relationships for R190E Slo2.1 channels recorded using the indicated extracellular solutions. Currents were recorded from the same oocyte as extracellular solution was changed in the order (from top to bottom) indicated in the symbol legend. Oocytes were recorded 1 d after injection with 0.84 ng cRNA (n = 8). After recording currents when oocytes were bathed in KCM211 and K104 solutions, oocytes were then incubated in Na_i-loading solution for 15 min before again measuring I-V relationship using K104 solution ("K104, Na_i-loaded"). Finally, the bathing solution was switched to KCM211, and currents were recorded once again ("KCM211, Na_i-loaded"). (B) Example of currents recorded from an oocyte before and after treatment with 1 mM NFA. Arrows indicate 0 current level. (C) I-V relationships for R190E Slo2.1 channels recorded from oocytes bathed in K104 extracellular solutions before and after treatment with 1 mM NFA. Oocytes were recorded 1 d after injection with 0.84 ng cRNA (n = 6). (D and E) I-V relationships for R190A (D) and R190Q (E) Slo2.1 channels recorded from oocytes bathed in K104 extracellular solutions before and after treatment with 1 mM NFA. Oocytes were recorded 1 d after injection with 0.92 ng R190A (n = 8) or 0.32 ng R190Q (n = 10) Slo2.1 cRNA.

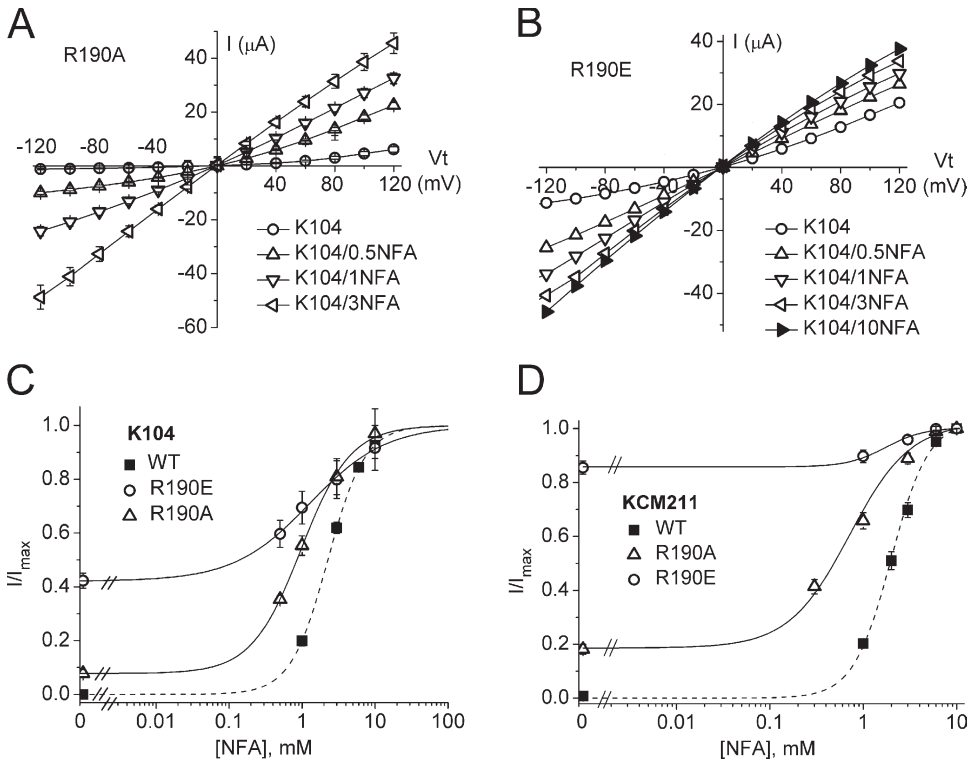

Figure 16. Concentration-dependent effects of NFA on R190A and R190E Slo2.1 channels. (A) I-V relationships for oocytes expressing R190A Slo2.1 channels and bathed in K104 solution. Oocytes were studied 2 d after injection of 0.84 ng cRNA ($n = 9$). (B) I-V relationships for oocytes expressing R190A Slo2.1 channels and bathed in K104 solution. Oocytes were studied 2 d after injection of 0.84 ng cRNA ($n = 6$). (C) Concentration–response relationships for oocytes expressing WT, R190A, or R190E Slo2.1 channels and bathed in K104 extracellular solution. Currents were measured at a V_t of +80 mV. The data were fitted with a modified Hill equation (smooth curves) to estimate EC_{50} and n_H values as follows: WT: $EC_{50} = 2.24 \pm 0.02$ mM and $n_H = 1.73 \pm 0.02$; R190E: $EC_{50} = 1.28 \pm 0.09$ and $n_H = 0.83 \pm 0.06$; R190A: $EC_{50} = 0.97 \pm 0.02$ and $n_H = 1.28 \pm 0.04$. (D) Concentration–response relationships for oocytes expressing WT, R190A, or R190E Slo2.1 channels and bathed in KCM211 extracellular solution. Currents were measured at a V_t of 0 mV. Hill equation parameters were as follows: WT: $EC_{50} = 2.1 \pm 0.87$ mM and $n_H = 1.74 \pm 0.50$; R190E: $EC_{50} = 1.98 \pm 0.43$ and $n_H = 2.15 \pm 0.80$; R190A: $EC_{50} = 0.71 \pm 0.13$ and $n_H = 1.34 \pm 0.24$. For C and D, currents were normalized to the extrapolated maximum response for each cell (I/I_{max}).

filter (SF). Their absence may induce a change in the configuration of the SF similar to the low K^+ structure for the bacterial KcsA channel that was proposed to disfavor ion conductance (Zhou et al., 2001). Although extracellular Na^+ does not alter inward currents, excessive elevation of intracellular Na^+ blocks outward currents, resulting in a region of negative slope conductance at very positive test potentials. Thus, elevated $[Na^+]_i$ has opposing effects on Slo2.1 channel activity, causing an increase in P_o and pore block.

Although the binding site for intracellular Na^+ has not been identified, it is assumed that similar to Ca^{2+} regulation of Slo1 channels, Na^+ binds to a specific region of the C terminus of Slo2.1 to cause the channels to open. Activation of channels by elevated $[Na^+]_i$ could result from a direct effect on an intracellular gate formed by the S6 bundle crossing, an allosteric effect on an extracellular gate formed by the SF/pore helix (PH), or by affecting both of these putative gating structures by a positively cooperative mechanism as recently proposed for K_{2P} leak channels (Ben-Abu et al., 2009). Based on several findings reported here, we propose that NFA mediates a change in the P_o of the SF/PH gate. First, extracellular applied NFA activates channels in the absence of intracellular Na^+. Second, NFA causes a concentration-dependent stabilization of channels in the open state, manifest as a shift of the voltage dependence of current activation to more negative potentials, and an increase in G/G_{max}, the minimum value of relative whole cell conductance. Third, in the presence of a saturating concentration of NFA, currents are time independent and channels are activated independently of transmembrane voltage, suggesting that NFA uncouples channel activation from voltage sensing. Fourth, neutralization of the charged residues in S1–S4, the typical VSD of Kv channels, does not affect the voltage dependence of Slo2.1. Finally, the potential importance of the SF/PH in the gating of Slo2.1 is suggested by the observed effects of $[K^+]_e$ on channel activity. The $V_{1/2}$ for activation was shifted to more positive potentials (opposite to NFA), as $[K^+]_e$ was elevated from 1 to 300 mM, with an EC_{50} value of 21.2 mM. The shift in $V_{1/2}$ is not predicted by the GHK current equation, and $[K^+]_e$ does not affect the voltage dependence of gating of Kv channels that is mediated by the opening and closing of the S6 bundle crossing gate (Yellen, 1998). For example, an increase in $[K^+]_e$ from 2 to 98 mM does not shift the voltage dependence of activation of hERG (S. Wang et al., 1997) and causes only a small hyperpolarizing shift in Kv4.3 (Wang et al., 2004). However, elevated $[K^+]_e$ alters C-type inactivation gating of Kv channels (Baukrowitz and Yellen, 1995), presumably mediated by changes in the configuration of the SF (Loots and Isacoff, 1998). In contrast to the effects of $[K^+]_e$ on the G-V relationship of

Slo2.1 channels, elevated $[K^+]_e$ increases the P_o of Kv channels at any given voltage (by shifting the voltage dependence of C-type inactivation to more positive potentials). Thus, the affect of $[K^+]_e$ on the conductance of Slo2.1 channels appears to be opposite to that observed for Kv channels that exhibit a C-type inactivation mechanism.

Mutation of charged residues in the S1–S4 segments of Slo2.1 did not significantly alter basal channel activity or outward rectification of the I-V relationship; however, nonconservative mutations of R190, a charged residue located either at the C-terminal end of S4 or at the N-terminal end of the S4–S5 linker, induced constitutive channel opening. Channels harboring a neutralizing mutation (R190A and R190Q) were open under basal conditions (normal $[Na^+]_i$, no NFA) and were more sensitive to activation by NFA (lower EC_{50} than WT channels) when $[K^+]_e$ was low. In the presence of high extracellular K^+ (i.e., K104 solution), the basal activity of R190A and R190Q channels was barely detectable, but channels still retained their increased sensitivity to NFA. Channels harboring a charge-reversing substitution (R190E) exhibited the greatest basal activity and were not further activated by NFA or Na_i loading when $[K^+]_e$ was low. However, Na_i-loading solution or NFA application increased R190E channel activity in the presence of high extracellular K^+ (K104 solution). These observations are consistent with the proposal that elevated $[K^+]_e$ decreases channel P_o.

The location of R190 in the Slo2.1 channel subunit is equivalent to D540 in hERG1. Charge-reversing mutations of D540 (e.g., K540) disrupt the closed state and promote the opening of hERG1 channels at very negative potentials by interacting with residues in the S6 segment of an adjacent subunit (Sanguinetti and Xu, 1999; Tristani-Firouzi et al., 2002; Ferrer et al., 2006). By homology, E190 might also interact with the putative S6 bundle crossing gate in Slo2.1 and cause an increase in channel P_o under basal conditions. Our findings on the effects of $[K^+]_e$, NFA, and R190 mutations on Slo2.1 conductance suggest that the S6 bundle crossing located at the intracellular end of the pore may not function as the sole activation gate that controls ion entry into the central cavity, as described for KcsA and MthK (Doyle et al., 1998; Liu et al., 2001; Jiang et al., 2002a,b) or Kv channels (Liu et al., 1997; Jiang et al., 2003; Long et al., 2005). Instead, we propose that Slo2.1 channel gating resembles CNG channels, where accumulating evidence indicates that the SF also functions as an activation gate. Although the configuration of the S6 bundle crossing in CNG channels changes in a voltage-dependent manner sufficient to gate the entry of large molecules such as MTSET into the central cavity, entry of small ions such as Ag^+ are not affected (Flynn and Zagotta, 2001). SF-mediated gating has also been proposed for $K_{Ca3.1}$ (Klein et al., 2007) and Slo1 (Wilkens and Aldrich, 2006) channels (but see Tang et al., 2009). Recent studies based on Ag^+ accessibility of Cys residues of CNG channels suggest that the PH (Liu and Siegelbaum, 2000) and SF (Contreras et al., 2008) change their configuration in response to cyclic nucleotide binding to the distant CNBD of the C terminus. It is unclear how ligand binding to the C terminus of CNG channels is converted to changes in the structure of the SF, but the S6 segments are the likely transducing element (Johnson and Zagotta, 2001; Nair et al., 2006; Mazzolini et al., 2009). A similar positive cooperativity between the intracellular (S6 bundle crossing) and extracellular (SF/PH) gates may explain how binding of extracellular NFA or intracellular Na^+ can independently increase the P_o of Slo2.1 channels.

We thank Kam Hoe Ng for oocyte isolation and injections.

This work was supported by a grant from the Nora Eccles Treadwell Foundation.

Christopher Miller served as editor.

Submitted: 17 August 2009
Accepted: 5 February 2010

REFERENCES

Adelman, J.P., K.Z. Shen, M.P. Kavanaugh, R.A. Warren, Y.N. Wu, A. Lagrutta, C.T. Bond, and R.A. North. 1992. Calcium-activated potassium channels expressed from cloned complementary DNAs. *Neuron.* 9:209–216. doi:10.1016/0896-6273(92)90160-F

Aggarwal, S.K., and R. MacKinnon. 1996. Contribution of the S4 segment to gating charge in the *Shaker* K^+ channel. *Neuron.* 16:1169–1177. doi:10.1016/S0896-6273(00)80143-9

Akera, T., R.H. Gubitz, T.M. Brody, and T. Tobin. 1979. Effects of monovalent cations on $(Na^+ + K^+)$-ATPase in rat brain slices. *Eur. J. Pharmacol.* 55:281–292. doi:10.1016/0014-2999(79)90196-1

Bader, C.R., L. Bernheim, and D. Bertrand. 1985. Sodium-activated potassium current in cultured avian neurones. *Nature.* 317:540–542. doi:10.1038/317540a0

Baukrowitz, T., and G. Yellen. 1995. Modulation of K^+ current by frequency and external $[K^+]$: a tale of two inactivation mechanisms. *Neuron.* 15:951–960. doi:10.1016/0896-6273(95)90185-X

Ben-Abu, Y., Y. Zhou, N. Zilberberg, and O. Yifrach. 2009. Inverse coupling in leak and voltage-activated K+ channel gates underlies distinct roles in electrical signaling. *Nat. Struct. Mol. Biol.* 16:71–79. doi:10.1038/nsmb.1525

Bhattacharjee, A., W.J. Joiner, M. Wu, Y. Yang, F.J. Sigworth, and L.K. Kaczmarek. 2003. Slick (Slo2.1), a rapidly-gating sodium-activated potassium channel inhibited by ATP. *J. Neurosci.* 23:11681–11691.

Busch, A.E., T. Herzer, C.A. Wagner, F. Schmidt, G. Raber, S. Waldegger, and F. Lang. 1994. Positive regulation by chloride channel blockers of IsK channels expressed in *Xenopus* oocytes. *Mol. Pharmacol.* 46:750–753.

Contreras, J.E., D. Srikumar, and M. Holmgren. 2008. Gating at the selectivity filter in cyclic nucleotide-gated channels. *Proc. Natl. Acad. Sci. USA.* 105:3310–3314. doi:10.1073/pnas.0709809105

Doyle, D.A., J. Morais Cabral, R.A. Pfuetzner, A. Kuo, J.M. Gulbis, S.L. Cohen, B.T. Chait, and R. MacKinnon. 1998. The structure of the potassium channel: molecular basis of K^+ conduction and selectivity. *Science.* 280:69–77. doi:10.1126/science.280.5360.69

Dryer, S.E. 1991. $Na^{(+)}$-activated K^+ channels and voltage-evoked ionic currents in brain stem and parasympathetic neurones of the chick. *J. Physiol.* 435:513–532.

Dryer, S.E. 1994. $Na^{(+)}$-activated K^+ channels: a new family of large-conductance ion channels. *Trends Neurosci.* 17:155–160. doi:10.1016/0166-2236(94)90093-0

Egan, T.M., D. Dagan, J. Kupper, and I.B. Levitan. 1992a. $Na^{(+)}$-activated K^+ channels are widely distributed in rat CNS and in *Xenopus* oocytes. *Brain Res.* 584:319–321. doi:10.1016/0006-8993(92)90913-T

Egan, T.M., D. Dagan, J. Kupper, and I.B. Levitan. 1992b. Properties and rundown of sodium-activated potassium channels in rat olfactory bulb neurons. *J. Neurosci.* 12:1964–1976.

Fernandez, D., J. Sargent, F.B. Sachse, and M.C. Sanguinetti. 2008. Structural basis for ether-a-go-go-related gene K^+ channel subtype-dependent activation by niflumic acid. *Mol. Pharmacol.* 73:1159–1167. doi:10.1124/mol.107.043505

Ferrer, T., J. Rupp, D.R. Piper, and M. Tristani-Firouzi. 2006. The S4-S5 linker directly couples voltage sensor movement to the activation gate in the human ether-a'-go-go-related gene (hERG) K^+ channel. *J. Biol. Chem.* 281:12858–12864. doi:10.1074/jbc.M513518200

Flynn, G.E., and W.N. Zagotta. 2001. Conformational changes in S6 coupled to the opening of cyclic nucleotide-gated channels. *Neuron.* 30:689–698. doi:10.1016/S0896-6273(01)00324-5

Goldin, A.L. 1991. Expression of ion channels by injection of mRNA into *Xenopus* oocytes. *Methods Cell Biol.* 36:487–509. doi:10.1016/S0091-679X(08)60293-9

Goldman, D.E. 1943. Potential, impedance, and rectification in membranes. *J. Gen. Physiol.* 27:37–60. doi:10.1085/jgp.27.1.37

Greenwood, I.A., and W.A. Large. 1995. Comparison of the effects of fenamates on Ca-activated chloride and potassium currents in rabbit portal vein smooth muscle cells. *Br. J. Pharmacol.* 116:2939–2948.

Gribkoff, V.K., J.T. Lum-Ragan, C.G. Boissard, D.J. Post-Munson, N.A. Meanwell, J.E. Starrett Jr., E.S. Kozlowski, J.L. Romine, J.T. Trojnacki, M.C. Mckay, et al. 1996. Effects of channel modulators on cloned large-conductance calcium-activated potassium channels. *Mol. Pharmacol.* 50:206–217.

Haimann, C., and C.R. Bader. 1989. Sodium-activated potassium channel in avian sensory neurons. *Cell Biol. Int. Rep.* 13:1133–1139. doi:10.1016/0309-1651(89)90027-1

Haimann, C., L. Bernheim, D. Bertrand, and C.R. Bader. 1990. Potassium current activated by intracellular sodium in quail trigeminal ganglion neurons. *J. Gen. Physiol.* 95:961–979. doi:10.1085/jgp.95.5.961

Haimann, C., J. Magistretti, and B. Pozzi. 1992. Sodium-activated potassium current in sensory neurons: a comparison of cell-attached and cell-free single-channel activities. *Pflugers Arch.* 422:287–294. doi:10.1007/BF00376215

Hamill, O.P., A. Marty, E. Neher, B. Sakmann, and F.J. Sigworth. 1981. Improved patch-clamp techniques for high-resolution current recording from cells and cell-free membrane patches. *Pflugers Arch.* 391:85–100. doi:10.1007/BF00656997

Harvey, R.D., and R.E. Ten Eick. 1989. On the role of sodium ions in the regulation of the inward-rectifying potassium conductance in cat ventricular myocytes. *J. Gen. Physiol.* 94:329–348. doi:10.1085/jgp.94.2.329

Hille, B., and W. Schwarz. 1978. Potassium channels as multi-ion single-file pores. *J. Gen. Physiol.* 72:409–442. doi:10.1085/jgp.72.4.409

Hodgkin, A.L., and B. Katz. 1949. The effects of sodium on the electrical activity of the giant axon of the squid. *J. Physiol.* 108:37–77.

Horrigan, F.T., J. Cui, and R.W. Aldrich. 1999. Allosteric voltage gating of potassium channels I. Mslo ionic currents in the absence of Ca^{2+}. *J. Gen. Physiol.* 114:277–304. doi:10.1085/jgp.114.2.277

Jiang, Y., A. Lee, J. Chen, M. Cadene, B.T. Chait, and R. MacKinnon. 2002a. Crystal structure and mechanism of a calcium-gated potassium channel. *Nature.* 417:515–522. doi:10.1038/417515a

Jiang, Y., A. Lee, J. Chen, M. Cadene, B.T. Chait, and R. MacKinnon. 2002b. The open pore conformation of potassium channels. *Nature.* 417:523–526. doi:10.1038/417523a

Jiang, Y., A. Lee, J. Chen, V. Ruta, M. Cadene, B.T. Chait, and R. MacKinnon. 2003. X-ray structure of a voltage-dependent K^+ channel. *Nature.* 423:33–41. doi:10.1038/nature01580

Johnson, J.P. Jr., and W.N. Zagotta. 2001. Rotational movement during cyclic nucleotide-gated channel opening. *Nature.* 412:917–921. doi:10.1038/35091089

Kameyama, M., M. Kakei, R. Sato, T. Shibasaki, H. Matsuda, and H. Irisawa. 1984. Intracellular Na^+ activates a K^+ channel in mammalian cardiac cells. *Nature.* 309:354–356. doi:10.1038/309354a0

Klein, H., L. Garneau, U. Banderali, M. Simoes, L. Parent, and R. Sauvé. 2007. Structural determinants of the closed KCa3.1 channel pore in relation to channel gating: results from a substituted cysteine accessibility analysis. *J. Gen. Physiol.* 129:299–315. doi:10.1085/jgp.200609726

Liu, J., and S.A. Siegelbaum. 2000. Change of pore helix conformational state upon opening of cyclic nucleotide-gated channels. *Neuron.* 28:899–909. doi:10.1016/S0896-6273(00)00162-8

Liu, Y., M. Holmgren, M.E. Jurman, and G. Yellen. 1997. Gated access to the pore of a voltage-dependent K^+ channel. *Neuron.* 19:175–184. doi:10.1016/S0896-6273(00)80357-8

Liu, Y.S., P. Sompornpisut, and E. Perozo. 2001. Structure of the KcsA channel intracellular gate in the open state. *Nat. Struct. Biol.* 8:883–887. doi:10.1038/nsb1001-883

Long, S.B., E.B. Campbell, and R. Mackinnon. 2005. Crystal structure of a mammalian voltage-dependent Shaker family K^+ channel. *Science.* 309:897–903. doi:10.1126/science.1116269

Loots, E., and E.Y. Isacoff. 1998. Protein rearrangements underlying slow inactivation of the Shaker K^+ channel. *J. Gen. Physiol.* 112:377–389. doi:10.1085/jgp.112.4.377

Luk, H.-N., and E. Carmeliet. 1990. $Na^{(+)}$-activated K^+ current in cardiac cells: rectification, open probability, block and role in digitalis toxicity. *Pflugers Arch.* 416:766–768. doi:10.1007/BF00370627

Ma, Z., X.J. Lou, and F.T. Horrigan. 2006. Role of charged residues in the S1-S4 voltage sensor of BK channels. *J. Gen. Physiol.* 127:309–328. doi:10.1085/jgp.200509421

Malykhina, A.P., F. Shoeb, and H.I. Akbarali. 2002. Fenamate-induced enhancement of heterologously expressed HERG currents in Xenopus oocytes. *Eur. J. Pharmacol.* 452:269–277. doi:10.1016/S0014-2999(02)02330-0

Mazzolini, M., C. Anselmi, and V. Torre. 2009. The analysis of desensitizing CNGA1 channels reveals molecular interactions essential for normal gating. *J. Gen. Physiol.* 133:375–386. doi:10.1085/jgp.200810157

McCormack, K., M.A. Tanouye, L.E. Iverson, J.W. Lin, M. Ramaswami, T. McCormack, J.T. Campanelli, M.K. Mathew, and B. Rudy. 1991. A role for hydrophobic residues in the voltage-dependent gating of Shaker K^+ channels. *Proc. Natl. Acad. Sci. USA.* 88:2931–2935. doi:10.1073/pnas.88.7.2931

Nair, A.V., M. Mazzolini, P. Codega, A. Giorgetti, and V. Torre. 2006. Locking CNGA1 channels in the open and closed state. *Biophys. J.* 90:3599–3607. doi:10.1529/biophysj.105.073346

Niu, X.W., and R.W. Meech. 2000. Potassium inhibition of sodium-activated potassium ($K_{(Na)}$) channels in guinea-pig ventricular myocytes. *J. Physiol.* 526:81–90. doi:10.1111/j.1469-7793.2000.00081.x

Noma, A. 1983. ATP-regulated K^+ channels in cardiac muscle. *Nature.* 305:147–148. doi:10.1038/305147a0

Ohmori, H. 1978. Inactivation kinetics and steady-state current noise in the anomalous rectifier of tunicate egg cell membranes. *J. Physiol.* 281:77–99.

Ottolia, M., and L. Toro. 1994. Potentiation of large conductance K_{Ca} channels by niflumic, flufenamic, and mefenamic acids. *Biophys. J.* 67:2272–2279. doi:10.1016/S0006-3495(94)80712-X

Peretz, A., N. Degani, R. Nachman, Y. Uziyel, G. Gibor, D. Shabat, and B. Attali. 2005. Meclofenamic acid and diclofenac, novel templates of KCNQ2/Q3 potassium channel openers, depress cortical neuron activity and exhibit anticonvulsant properties. *Mol. Pharmacol.* 67:1053–1066. doi:10.1124/mol.104.007112

Robinson, J.D. 1975. Mechanisms by which Li+ stimulates the (Na^+ and K^+)-dependent ATPase. *Biochim. Biophys. Acta.* 413:459–471. doi:10.1016/0005-2736(75)90129-7

Rodrigo, G.C., and R.A. Chapman. 1990. A sodium-activated potassium current in intact ventricular myocytes isolated from the guinea-pig heart. *Exp. Physiol.* 75:839–842.

Safronov, B.V., and W. Vogel. 1996. Properties and functions of $Na(^+)$-activated K^+ channels in the soma of rat motoneurones. *J. Physiol.* 497:727–734.

Sanguinetti, M.C. 1990. Na^+-activated and ATP-sensitive K^+ channels in the heart. *In* Potassium Channels: Basic Function and Therapeutic Aspects. T. Colatsky, editor. Alan R. Liss, Inc., New York. 85–110.

Sanguinetti, M.C., and Q.P. Xu. 1999. Mutations of the S4-S5 linker alter activation properties of HERG potassium channels expressed in *Xenopus* oocytes. *J. Physiol.* 514:667–675. doi:10.1111/j.1469-7793.1999.667ad.x

Santi, C.M., G. Ferreira, B. Yang, V.R. Gazula, A. Butler, A. Wei, L.K. Kaczmarek, and L. Salkoff. 2006. Opposite regulation of Slick and Slack K^+ channels by neuromodulators. *J. Neurosci.* 26:5059–5068. doi:10.1523/JNEUROSCI.3372-05.2006

Schreiber, M., A. Wei, A. Yuan, J. Gaut, M. Saito, and L. Salkoff. 1998. Slo3, a novel pH-sensitive K^+ channel from mammalian spermatocytes. *J. Biol. Chem.* 273:3509–3516. doi:10.1074/jbc.273.6.3509

Seoh, S.-A., D. Sigg, D.M. Papazian, and F. Bezanilla. 1996. Voltage-sensing residues in the S2 and S4 segments of the *Shaker* K^+ channel. *Neuron.* 16:1159–1167. doi:10.1016/S0896-6273(00)80142-7

Stühmer, W. 1992. Electrophysiological recording from *Xenopus* oocytes. *Methods Enzymol.* 207:319–339. doi:10.1016/0076-6879(92)07021-F

Tamsett, T.J., K.E. Picchione, and A. Bhattacharjee. 2009. NAD^+ activates K_{Na} channels in dorsal root ganglion neurons. *J. Neurosci.* 29:5127–5134. doi:10.1523/JNEUROSCI.0859-09.2009

Tang, Q.Y., X.H. Zeng, and C.J. Lingle. 2009. Closed-channel block of BK potassium channels by bbTBA requires partial activation. *J. Gen. Physiol.* 134:409–436. doi:10.1085/jgp.200910251

Tiwari-Woodruff, S.K., C.T. Schulteis, A.F. Mock, and D.M. Papazian. 1997. Electrostatic interactions between transmembrane segments mediate folding of Shaker K^+ channel subunits. *Biophys. J.* 72:1489–1500. doi:10.1016/S0006-3495(97)78797-6

Tiwari-Woodruff, S.K., M.A. Lin, C.T. Schulteis, and D.M. Papazian. 2000. Voltage-dependent structural interactions in the *Shaker* K^+ channel. *J. Gen. Physiol.* 115:123–138. doi:10.1085/jgp.115.2.123

Tristani-Firouzi, M., J. Chen, and M.C. Sanguinetti. 2002. Interactions between S4-S5 linker and S6 transmembrane domain modulate gating of HERG K^+ channels. *J. Biol. Chem.* 277:18994–19000. doi:10.1074/jbc.M200410200

Vasilets, L.A., H.S. Omay, T. Ohta, S. Noguchi, M. Kawamura, and W. Schwarz. 1991. Stimulation of the Na^+/K^+ pump by external $[K^+]$ is regulated by voltage-dependent gating. *J. Biol. Chem.* 266:16285–16288.

Wang, H.S., J.E. Dixon, and D. McKinnon. 1997. Unexpected and differential effects of Cl- channel blockers on the Kv4.3 and Kv4.2 K^+ channels. Implications for the study of the $I(_{to2})$ current. *Circ. Res.* 81:711–718.

Wang, S., S. Liu, M.J. Morales, H.C. Strauss, and R.L. Rasmusson. 1997. A quantitative analysis of the activation and inactivation kinetics of HERG expressed in *Xenopus* oocytes. *J. Physiol.* 502:45–60. doi:10.1111/j.1469-7793.1997.045bl.x

Wang, S., V.E. Bondarenko, Y. Qu, M.J. Morales, R.L. Rasmusson, and H.C. Strauss. 2004. Activation properties of Kv4.3 channels: time, voltage and $[K^+]_o$ dependence. *J. Physiol.* 557:705–717. doi:10.1113/jphysiol.2003.058578

Wang, Z., T. Kimitsuki, and A. Noma. 1991. Conductance properties of the Na(+)-activated K+ channel in guinea-pig ventricular cells. *J. Physiol.* 433:241–257.

Weber, W. 1999. Ion currents of *Xenopus laevis* oocytes: state of the art. *Biochim. Biophys. Acta.* 1421:213–233. doi:10.1016/S0005-2736(99)00135-2

White, M.M., and M. Aylwin. 1990. Niflumic and flufenamic acids are potent reversible blockers of $Ca^{2(+)}$-activated Cl^- channels in *Xenopus* oocytes. *Mol. Pharmacol.* 37:720–724.

Wilkens, C.M., and R.W. Aldrich. 2006. State-independent block of BK channels by an intracellular quaternary ammonium. *J. Gen. Physiol.* 128:347–364. doi:10.1085/jgp.200609579

Yellen, G. 1998. The moving parts of voltage-gated ion channels. *Q. Rev. Biophys.* 31:239–295. doi:10.1017/S0033583598003448

Yuan, A., C.M. Santi, A. Wei, Z.W. Wang, K. Pollak, M. Nonet, L. Kaczmarek, C.M. Crowder, and L. Salkoff. 2003. The sodium-activated potassium channel is encoded by a member of the Slo gene family. *Neuron.* 37:765–773. doi:10.1016/S0896-6273(03)00096-5

Zhainazarov, A.B., and B.W. Ache. 1997. Gating and conduction properties of a sodium-activated cation channel from lobster olfactory receptor neurons. *J. Membr. Biol.* 156:173–190. doi:10.1007/s002329900199

Zhou, Y., J.H. Morais-Cabral, A. Kaufman, and R. MacKinnon. 2001. Chemistry of ion coordination and hydration revealed by a K^+ channel-Fab complex at 2.0 A resolution. *Nature.* 414:43–48. doi:10.1038/35102009